Biocompatible and Biodegradable Light-Emitting Materials and Devices

Deying Kong, Kaiyuan Zhang, Jingjing Tian, Lan Yin,* and Xing Sheng*

Implantable devices with desirable biocompatibility and even degradability are of significant interest to biomedical communities. Biologically safe and resorbable electronic materials and devices have been extensively explored, and numerous biodegradable optical sensors, detectors, and waveguides have also been successfully demonstrated. However, biocompatible and degradable optical emitters, especially electrically driven ones, are relatively underexplored. This article provides an overview on the recent progress in the development of biocompatible and biodegradable light-emitting materials and devices. First, an introduction on molecular dyes, proteins, and inorganic particles with photoluminescence is provided. Subsequently, material systems with unusual optical properties including sonoluminescence, chemiluminescence, and bioluminescence are highlighted. Finally, electroluminescent materials and device with potential for fully biodegradation are emphasized upon. Upon success, it is envisioned that these biodegradable light-emitting materials and devices would provide effective and unique capabilities in broad biomedical applications from biological sensing and modulation to clinical diagnostics and therapy.

D. Kong, Prof. L. Yin
School of Materials Science and Engineering
The Key Laboratory of Advanced Materials
of Ministry of Education
State Key Laboratory of New Ceramics
and Fine Processing
Center for Flexible Electronics Technology
Tsinghua University
Beijing 100084, China
E-mail: lanyin@tsinghua.edu.cn
K. Zhang, Prof. X. Sheng
Department of Electronic Engineering
Beijing National Research Center for Information
Science and Technology
Center for Flexible Electronics Technology
IDG/McGovern Institute for Brain Research
Tsinghua University
Beijing 100084, China
E-mail: xingsheng@tsinghua.edu.cn
Dr. J. Tian
Department of Medical Science Research Center
Peking Union Medical College Hospital
Chinese Academy of Medical Sciences and Peking Union
Medical College
Beijing 100730, China

The ORCID identification number(s) for the author(s) of this article can be found under https://doi.org/10.1002/admt.202100006.

1. Introduction

Photon signals play critical roles in living systems, involving in a variety of processes including photosynthesis, circadian regulation, biomodulation, and bioluminescence.[1] Optical-based technologies have been widely employed in biomedical fields, for versatile applications such as biological sensing, fluorescence imaging, neural stimulation, and phototherapy.[2] For many applications in vivo, photons with specific wavelengths and certain power levels have to be delivered deep in animal bodies, in order to realize effective light and cell/tissue interactions. However, light propagation in the tissue is limited to less than a few millimeters (for visible light), due to strong scattering and absorption of biological tissues. Commonly used methods for light transmission within the body rely on implantable optical fibers or waveguides that are interconnected with external light sources.[3] These kinds of optical systems impose constraints for studying subjects and are associated with increased risks for infections.

Recently developed thin-film, microscale optoelectronic devices based on high performance semiconducting materials have shown great potential for biointegrated and biomimetic applications.[4] Via the assembly onto curved, flexible, stretchable, and biocompatible substrates, as well as the integration of wirelessly powered circuit units, these microdevices can be seamlessly attached on the human skin or injected into the animal body, with notable demonstrations on oximetry sensing, fluorescence imaging, optogenetic stimulation, and photodynamic therapy.[5,6] In particular, microdevice systems based on biocompatible materials that can fully dissolve within the animal body after operation and therefore eliminate second surgery for device retrieval, have attracted tremendous interests because of their potential as next-generation medical implants, which are also termed as "bioelectronic medicine" or "electroceuticals."[7] Examples of biodegradable materials include metals like magnesium (Mg), zinc (Zn), and iron (Fe),[8] and organic polymers like poly lactic-*co*-glycolic acid (PLGA), polycaprolactone (PCL), and hydrogels.[9,10] More recently, the discovery of the natural dissolution of silicon (Si) and germanium (Ge) thin films in biological environments opens the door to physically transient, functional electronic devices operating within the body.[11] These biocompatible and dissolvable metals, insulators and semiconductors establish the foundations for

the family of fully degradable electronic devices (diodes, transistors, electrodes, capacitors, inductors, etc.) and photonic devices (waveguides, photodetectors, plasmonic sensors, etc.).[12] In this existing portfolio of devices for "green electronics," one of the highly underdeveloped components is an electrically driven light emitter.[13] Currently, high-performance light-emitters are mostly based on III–V compound semiconductors,[14] lead (Pb) halide perovskites, or organic materials (small molecules and polymers).[15] These light emitting materials have been widely employed in fields of lighting and displays; however, they are nondegradable (for III–Vs) or even toxic (for Pb-based perovskites and some organics) when dissolving in the body. Therefore, it will be highly demanded to realize biocompatible and degradable light-emitting devices (like light-emitting diodes (LEDs) and lasers) with desirable emitting spectra and power densities. Such biodegradable light emitters can be integrated with other functional electronic systems, forming physically transient implants with unprecedented opportunities in biomedicine.

In this article, we review the context of biocompatible and biodegradable light-emitting materials and devices, focusing on their material compositions, device structures, optical properties, as well as specific biomedical applications. We begin with the discussion on photoluminescent materials, including fluorescent dyes, proteins, and quantum dots (QDs), followed by advanced materials with mechanoluminescence, chemiluminescence, and bioluminescence. Subsequent sections cover electroluminescent (EL) materials and devices, with various biocompatible or biodegradable active layers including organics made of small molecules and polymers, lead-free perovskites, and inorganic luminescence materials. Potential applications of these biocompatible and degradable emitters are highlighted, and their existing limitations are also discussed. We conclude with perspectives for fundamental research and translational applications in the future.

2. Materials with Photoluminescence (PL)

PL is a physical phenomenon of light emission upon absorbing incident light, which has a great potential for biomedical usage. The assessment of materials' biocompatibility and toxicity is critically important in the development of photoluminescence materials for biological integration. In recent years, a growing number of studies have focused on the biocompatible and biodegradable photoluminescence materials, which are mostly derived from conventional luminescent materials, such as dyes and proteins. Structurally designed luminescence materials such as quantum dot emitters have also been applied in the biological field. Here, we emphasize on biocompatible photoluminescence materials based on dyes, proteins, and inorganic particles.

2.1. Dye Molecules

Fluorescent dyes are usually based on small organic molecules. Fluorescein and calcein are typical fluorescent dyes commonly used in fundamental biology studies, but not widely used for in vivo applications, because of their poor photostability and cytotoxicity.[16] In order to address the issue of biological toxicity, nontoxic fluorescent dyes have been actively investigated. As an example shown in **Figure 1**a, a series of biodegradable fluorescent films prepared from regenerated cellulose (RC) films and fluorescent dyes (fluorescein, Acridine Orange, Rhodamine B, PLB-7C, or PLO-8C), with spectra shown the fluorescent properties.[17] Additionally, dyes and molecules can be embedded into hydrogels to form injectable bioscaffolds with fluorescent imaging capability. Tsou et al. developed a dopant-free photoluminescent hydrogels formed by in situ crosslinking of biocompatible polymer precursors.[18] The polycondensation reaction of citric acid and hexaethylene glycol is used to prepare photoluminescent oligomers (CHPO), followed by the connection of serine or cysteine and ethyl ester of a thiol acid to obtain oligomers (CHPO-Ser-ET and CHPO-Cys-ET). Images and optical properties of these hydrogels are presented in Figure 1b. When excited with two different wavelengths (365 and 488 nm), the two hydrogels exhibit similar PL spectral peaks but different intensities. Given desirable biodegradability, mechanical properties, and fluorescence characteristics, these fluorescent hydrogels can be made into implantable drug carriers, cellular scaffolds and imaging probes. In other works, the control of emission spectra is achieved by varied chemical synthesizations. Du et al. developed a poly(silicone-citrate) (PSC) hybrid polymer, as shown in Figure 1c.[19] Poly(citrate) (PC) elastomers possess advantages such as biocompatibility, biodegradability, and ideal mechanical behaviors that match with soft tissues. The PL intensity can be adjusted with varied material compositions. The crosslinked elastomers PC(CPC) and PSC(CPSC) with different silicone-citrate ratios 0.2:1.0 and 0.4:1.0 were denoted as CPSC(0.2) and CPSC(0,4), respectively. These elastomers show stable light output but different PL efficiencies. In all, molecular fluorescent dyes have attracted considerable interest because of their small molecular weight and facile synthesis. However, these molecular dyes show certain cytotoxicity that is associated with aromatic groups and hinders their applications for in vivo medical implants. Other limitations come from their low photobleaching thresholds and lack of functional groups for conjugation. To address these issues, possible solutions involve exploring new nontoxic fluorescent molecules derived from natural living systems, and the incorporation with biodegradable polymers to improve biocompatibility.

2.2. Protein

Fluorescent proteins are widely used in biological sensing and imaging. In 1956, Shimomura et al. first obtained green fluorescence protein (GFP) from *Aequorea victoria* jellyfish (**Figure 2**a). Chalfie et al. measured excitation and emission spectra of GFP expressed in *Escherichia coli* bacteria and purified *A. victoria* L form GFP, indicating the GFP can be expressed in different living cells.[20] Until now, GFPs and their derivatives are still among the most widely applied biological tools in biofluorescence imaging. As an example, the enhanced GFP (eGFP) produced from *E. coli* emits green fluorescence when excited by ultraviolet.[21] The highly efficient luminescence and biofriendly characteristics of eGFP has also
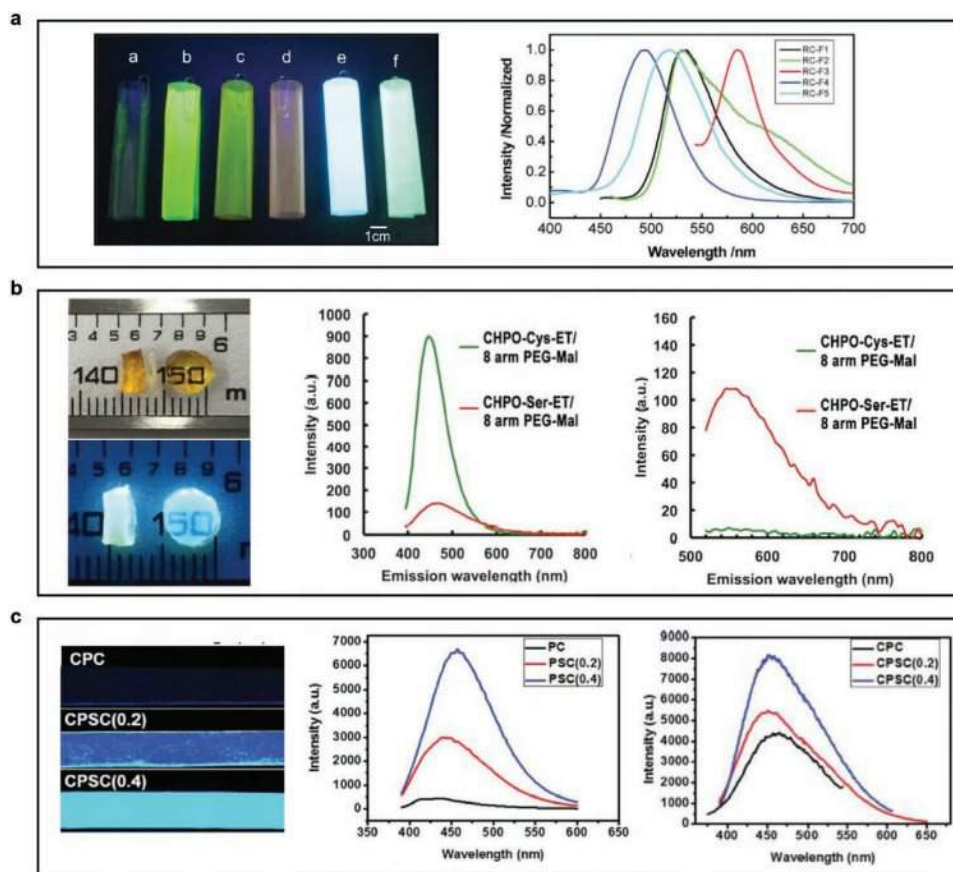
Figure 1. a) (Left) Images of RC films (a: RC; b: RC-fluorescein; c: RC-Acridine Orange; d: RC-Rhodamine B; e: RC-PLB-7C; f: RC-PLO-8C) excited under UV light (302 nm); (right) PL spectra of the corresponding films. Reproduced with permission.[17] Copyright 2009, The Royal Society of Chemistry. b) (Left) Images of CHPO-Ser-ET/eight-arm PEG-maleimide hydrogels under ambient light (top) and with excitation at 450 nm (bottom), and (middle and right) corresponding PL spectra emission spectra at excitations of 365 nm (middle) and 488 nm (right). Reproduced with permission.[18] Copyright 2018, Wiley-VCH. c) (Left) Fluorescent images of hybrid elastomers CPC, CPSC(0.2), and CPSC(0.4) under UV excitation (365 nm), and (middle and right) PL spectra of PSC in PC solutions and CPC hybrid elastomers (excited at 360 nm). Reproduced with permission.[19] Copyright 2015, Wiley-VCH.

enabled other interesting applications besides imaging. As shown in Figure 2b, Carlos et al. employed the eGFP to serve as an active absorber in luminescent solar concentrator (LSC) devices to improve the environmental friendliness of LSC.[21] Derived from GFPs, fluorescent proteins with different excitation and emission spectra are also being actively investigated and utilized for various imaging applications. For example, the cyan fluorescence protein (CFP) is obtained by adapting the environment of the tyrosine-based chromophore in the GFP to the tryptophan-based chromophore. It exhibits environmentally dependent optical characteristics, such as pH sensitivity. As shown in Figure 2c, CFP shows conformational differences in different pH environments, thereby different absorption spectra.[22] These fluorescent proteins not only present high luminous efficiencies but also ideal biocompatibilities. Moreover, they can be genetically encoded and expressed in living cells and organisms. When fused with different functional protein groups, they can be genetically modified for various detection capabilities (for example, calcium,[23] dopamine,[24] etc.) with a high sensitivity and selectivity. Conventionally considered to be purely optically excited luminophores, fluorescent proteins are not electronically active. Although fluorescent

protein cannot be directly energized to emit light, it can be used as a phosphor to convert light, for example, as a coating layer to realize a white LED.[25] To the best of our knowledge, there are no reports about the use of them as the active emitting layer in electrically driven devices.

2.3. Inorganic Nanoparticles (NPs)

Compared with organic-based dyes and proteins, inorganic-based NPs and QDs have advantages of high luminous brightness and stability. Their optical properties and biomedical applications have been extensively studied and reviewed in the literature,[26] and here we only highlight some recent examples. Carbon-based quantum dots (CDs) have attracted much attention because of their high aqueous solubility, robust chemical inertness, facile modification, and high resistance to photobleaching.[27] A variety of methods such as chemical ablation, electrochemical carbonization, hydrothermal/solvothermal treatment, laser ablation, and microware irradiation have been developed to synthesize CDs,[28] and these CDs can be functionalized by other biological materials to achieve various applications. For example,
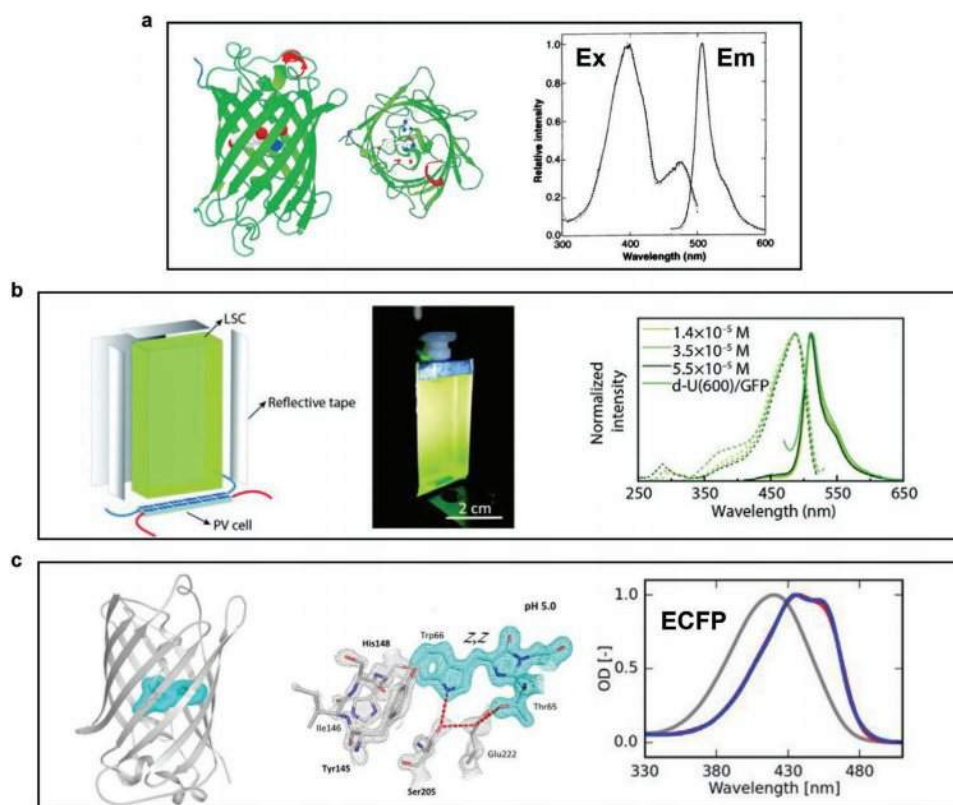
**ADVANCED
SCIENCE NEWS**
www.advancedsciencenews.com

**ADVANCED
MATERIALS
TECHNOLOGIES**
www.advmattechnol.de

Figure 2. a) (Left) Schematic illustration for the structure of GFP. Reproduced with permission.[20c] Copyright 2009, The Royal Society of Chemistry. (Right) Excitation and emission spectra of *E. coli*-generated GFP (solid lines) and purified *A. victoria* L form GFP (dotted lines). Reproduced with permission.[20d] Copyright 1994, Elsevier. b) (Left) Schematic of an eGFP-based luminescent solar concentrator (LSC), (middle) luminescent image of the eGFP LSC, and (right) excitation (dashed lines) and emission (solid lines) spectra of solutions of eGFP with different concentrations and doped d-U(600)/eGFP. Reproduced with permission.[21] Copyright 2020, The Royal Society of Chemistry. c) (Left) Scheme for the structure of ECFP, (middle) chromophore configuration and environment in ECFP, and (right) absorption spectra of ECFP. Reproduced with permission.[22] Copyright 2017, American Chemical Society.

Schneider et al. mixed citric acid with ethylenediamine to prepare CDs at elevated temperature that exhibit highly efficient blue light emission (centered at 450 nm) under ultraviolet (UV) illumination (**Figure 3**a).[29] Another example of biocompatible fluorescent NPs is zinc oxide (ZnO)-based nanocrystals. Because of its large bandgap as 3.3 eV, pure ZnO has an exciton induced transition induced PL emission in the UV range.[30] PL emissions of ZnO particles in the visible range are usually originated from radiative recombinations at defect states.[31] Dependent on experimental parameters for synthesis, the surface morphology, internal defects, and surface defects of ZnO can be modified and create different emission profiles in the visible region. Kocsis et al. adjusted the internal defect states of ZnO NPs by preparing them in different solvent environments. As shown in Figure 3b, the obtained ZnO NPs present different emission characteristics at different humidity and air pressure.[31] To apply these NPs in biological environments, many challenges have to be addressed, which are associated with their poor aqueous dispersion, instability of surface states, and biological rejection reactions. To offer better biocompatibility, biologically functional polymer groups can be assembled on the surface of NPs. An example of such surface modifications is provided in Figure 3c. Functional coatings on surfaces of ZnO-based QDs transform the originally hydrophobic surface into a hydrophilic surface.

In addition, the functionalized surfaces can be used to target on specific cells upon delivery by injection. These modified QDs with tunable emission wavelengths are utilized to exploit multispectral fluorescence imaging of cancer cells in vivo.[20a] However, such high-performance QDs have active cores made of ZnO, which prohibits their further applications for clinical trials. Future endeavors include the development of injectable NPs and QDs with high quantum yields, better biocompatibility, and versatile biological functionalities.[32] In addition, materials with emissions shifted to the biologically transparent window in the infrared range are highly desirable for imaging applications.[33] **Table 1** summarizes the optical properties of some representative photoluminescent biomaterials. Finally, electrically driven light-emitting devices (for example, quantum dot LEDs (QLEDs)) can be explored based on biocompatible electrodes and carrier injection layers, which will be covered in subsequent sections.

3. Materials with Sonoluminescence, Chemiluminescence, and Bioluminescence

In addition to those classical PL-based emissive materials discussed in preceding sections, photoemissions can be generated
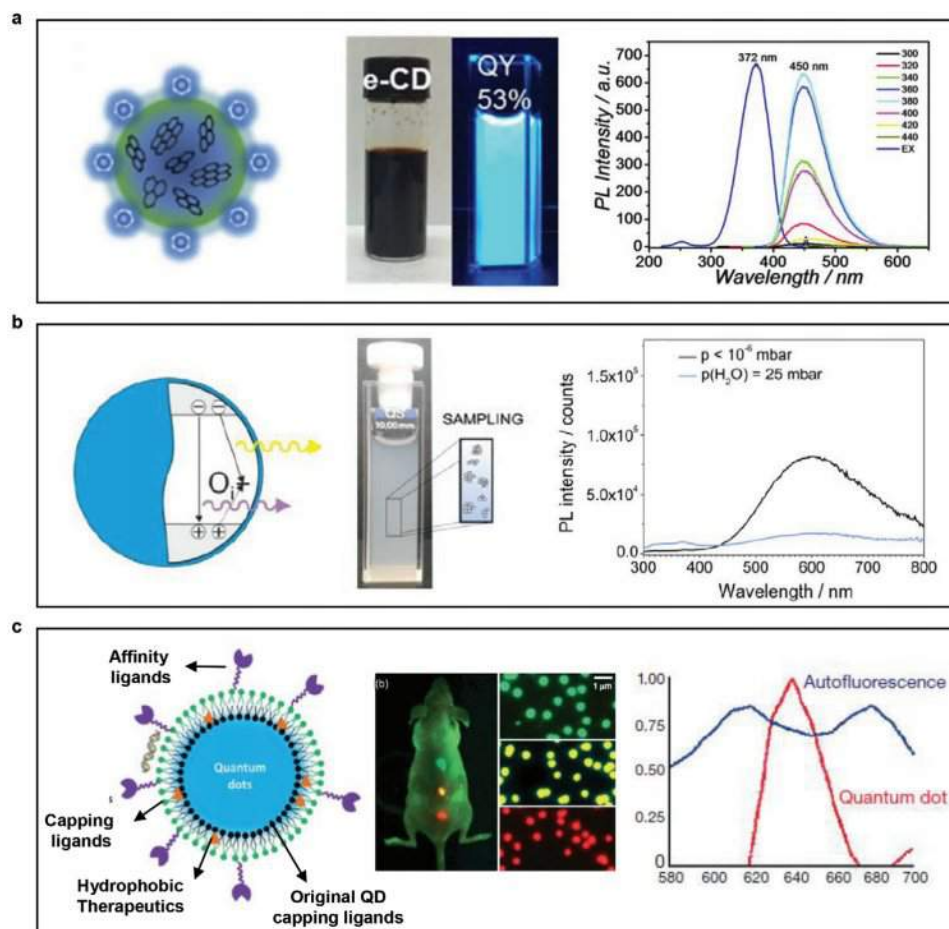
Figure 3. a) (Left) Schematic of citric acid-based carbon dots using EDA (e-CDs), (middle) photographs of solution with e-CDs under ambient and UV light, and (right) PL spectra of e-CDs under different excitations. Reproduced with permission.[29] Copyright 2016, American Chemical Society. b) (Left) Photoprocesses of ZnO nanoparticles (NPs), (middle) photo of ZnO NPs in aqueous dispersions, and (right) PL emission spectra of ZnO NPs in different environments. Reproduced with permission.[31a] Copyright 2016, Elsevier. c) (Left) Multifunctional quantum dots (QDs) coated with biodegradable polymers, (middle) QDs of different colors injected in a living mouse, and (right) PL spectra for animal skin with and without red QDs. Reproduced with permission.[31b] Copyright 2004, Nature Publishing Group.

by other excitation sources, including but not limited to, ultrasound, chemical reaction, and biological processes, with corresponding phenomena called sonoluminescence, chemiluminescence, and bioluminescence. Sonoluminescence is a process that converts mechanical energy generated by ultrasound into light waves. Such mechanically induced light emissions are advantageous for wireless power delivery in the deep tissue, because ultrasound waves have much larger penetration

Table 1. Material compositions and optical characteristics (excitation peak, emission peak, and quantum yield) for some representative photoluminescent materials.

Category	Fluorescent material	Excitation peak [nm]	Emission peak [nm]	Quantum yield [%]
Fluoresceins	RC films[17]	365	500–600	–
	CHPO-Ser/Cys-ET[18]	365 and 450	365 and 488	16, 36
	CPSC(0.4)[19]	360	452	35.5
Fluorescent proteins	Cerulean[20a]	Ultraviolet	475	62
	eGFP[21]	485	530	50
	ECFP[22]	430	400–500	36
Quantum dots	Carbon[28b]	320	≈450	7–51
	ZnO[30c]	320–532	400–800	30–85
	ZnS-capped CdSe[31b]	350–560	520 and 650	≈60

in the deep tissue (larger than ≈20 mm) than optical techniques (less than ≈1 mm) (**Figure 4**a).[34] Figure 4b presents an example of using ZnS:Ag NPs for ultrasound triggered optogenetic stimulation in the brain. These sonoluminescent NPs can enter the blood circulation by intravenous infusion and provide ultrasound triggered photon emission, acting as a local light source in the mouse brain.[35] Alternatively, light generation can be induced with energy created by chemical reactions. For example, chemiluminescence can be caused by the luminol reaction of oxalate and hydrogen peroxide.[36] Figure 4c presents results of chemiluminescence generated by NPs formed with bis[2,4,5-trichloro-6-(pentyloxycarbonyl)phenyl] oxalate (CPPO) and photosensitizer tetraphenylethylene-benzothiadiazole-dicyanovinyl (TBD),[37] which is C-TBD. Strong red light emission can be observed when this biocompatible NP reacts with hydrogen peroxide (H_2O_2), which can be used in tumor cells with high H_2O_2 concentration. When these NPs are in contact with tumor cells with a high H_2O_2 concentration, chemiluminescence occurs automatically to activate the photosensitive drug for the photodynamic therapy. Similar to chemiluminescence, bioluminescence is referred to autofluorescence generated in luminophores activated by biochemical processes. A common example is the bioluminescence of fireflies that is associated with the reaction of D-luciferin and adenosine

triphosphate (ATP) and oxygen (Figure 4d,e).[38] The oxidation progress emits light at 550 nm.

Moreover, Iwano et al. developed a new type of luciferase Akaluc through a mutant screening method, which increased the fluorescence intensity of luciferin AkaLumine-HCl 100–1000 times that of D-luciferin.[39] They used this tool to construct a new bioluminescence system in the body, and used this bioluminescence system to track cancer cells in mice and brain cell activity in monkeys. As for plants, Mitiouchkina et al. introduced bacterial luminescence genes into plants through genetic modification technology, and converted the ubiquitous caffeine in plants into fluorescein, thereby realizing plant luminescence.[40]

4. Electroluminescence Materials and Devices

Besides the aforementioned photoluminescent, sonoluminescent, chemiluminescent, and bioluminescent materials, EL devices such as LEDs are also attracting great attention for biomedical applications because of their high power conversion efficiency, longtime stability, electrical tunability, and easy integration with other electronic components. Conventional microscale LEDs made by III–V compound semiconductors
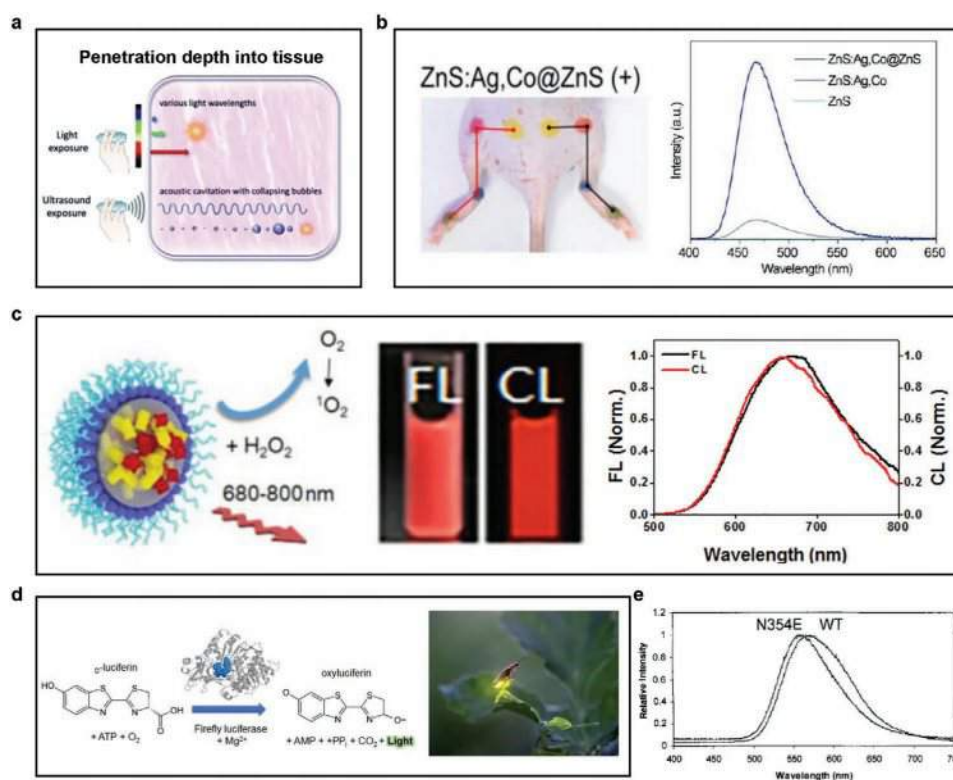

Figure 4. a) Schemes for mechanisms of the light and the ultrasound activated luminescence. Reproduced with permission.[34] Copyright 2020, The Royal Society of Chemistry. b) (Left) Image of a mouse during sono-optogenetic stimulation remotely after injecting ZnS:Ag,Co@ZnS NPs; (right) mechanoluminescence spectra of undoped ZnS (cyan), ZnS:Ag,Co (gray), and ZnS:Ag,Co@ZnS NPs (blue) under focused ultrasound excitation. Reproduced with permission.[35] Copyright 2019, Elsevier. c) (Left) Schematic for chemiluminescence of C-TBD NPs, (middle) fluorescence (FL) and chemiluminescence (CL) images of C-TBD NPs, and (right) FL and CL spectra of C-TBD NPs. Reproduced with permission.[37a] Copyright 2017, Elsevier. d) (Left) Scheme for bioluminescence (BL) with the luciferin–luciferase reaction, and (right) photograph of firefly with BL. Reproduced with permission.[38a] Copyright 2020, Regents of the University of California. e) BL spectra for luciferase in wild-type *Macrolampis* and the N354E substitution. Reproduced with permission.[38b] Copyright 2005, American Society for Photobiology.

**ADVANCED
SCIENCE NEWS**
www.advancedsciencenews.com

**ADVANCED
MATERIALS
TECHNOLOGIES**
www.advmattechnol.de

(gallium arsenide GaAs, gallium nitride GaN, etc.) have been extensively used as wearable and implantable light sources in biomedicine.[5,41] However, these semiconductors are rigid, non-degradable, and even contain toxic elements (e.g., As), making them undesirable as implantable devices for potential medical usage. It is both scientifically intriguing and clinically relevant if we can realize high-performance LEDs with active emitting layers, carrier transfer layers, electrodes, and substrates made of fully biocompatible and even biodegradable materials, which so far have not been reported. This section reviews recent progresses on EL devices based on organic molecules, polymers, Pb-free perovskites, and other semiconductors, which provides possible routes toward the path.

4.1. Organic Light-Emitting Materials and Devices

Organic light-emitting diodes (OLEDs) contain small organic molecule-based emitters, hole/electron transfer/blocking layers, electrodes, and substrates that can possibly be replaced by biocompatible and degradable materials. Traditional OLEDs employ active molecules compromising biohazardous groups like benzene and anthracene, which can be replaced by materials with better biocompatibility. **Table 2** summarizes some representative bioderived materials that can be applied in OLEDs as functional structural layers and their associated device performance. EL properties for typical bioderived materials like chlorophyll a, cytochrome c, myoglobin, hemin, and vitamin B12 have been reported.[42] **Figure 5**a presents an example of such OLEDs made with junctions of ITO/cytochrome c/Al. Unlike conventional OLEDs, the device exhibits a broadband emission with low quantum yields, partly due to the simple device structure without properly designed electron and hole transport layers.

A schematic energy diagram model is developed to explain the optoelectronic properties of such devices, and demonstrates that the corresponding emission and absorption spectra directly reflect the optical transition probability while some transitions are forbidden in biomolecules containing transition metals. Further efforts have been explored to improve the performance of these bioderived OLEDs, for example, by adjusting the molecular structures and optimizing device configurations. For example, by mixing the chlorophylls-based active emitter in a poly[(*m*-phenylenevinylene)-alt-(2,5-dihexyloxy-*p*-phenylenevinylene)] (PPV) host material, the concentration related quenching effect could be mitigated, thereby improving the radiative efficiency of chlorophylls. In addition, the EL device is found to exhibit a longer life time when containing antioxidant carotenoids, owing to the diminished oxidation damage of chlorophylls.[43] With Tri-*n*-propylamine (TPrA) as a coreactant, luminous efficiency of natural chlorophyll a can be further improved, realizing electrogenerated chemiluminescent sensing capability.[44] Figure 5b presents an efficient riboflavin-based OLED and its corresponding spectra.[45] By tailoring the sidegroups of riboflavin, the bioderived riboflavin tetrabutyrate (RFLT) shows significantly enhanced photoemissions associated with direct transition between the highest occupied molecular orbital (HOMO) and the lowest unoccupied molecular orbital (LUMO). Furthermore, a poly(9-vinylcarbazole) (PVK)-based hole injection layer is employed to further improve the EL efficiency with induced PVK-RFLT exciplex. Flavins could also achieve other desired functions including absorption and emission peaks red shift with proper chemical modifications.[46]

Apart from the active emitting layers, carrier transfer and blocking layers are critically important for high performance OLEDs as well, since the balance of electron and hole injection rates significantly affects the device EL efficiency. DNA-based

Table 2. Applications of some bioderived materials in OLEDs and corresponding device structures and properties.

Biomaterials in OLEDs	Layer function	Full OLED device structure	EQE [%]	EL emission peak [nm]	Refs.
Chlorophyll a	Emitter	ITO/chlorophyll a/Al	$1.6 \times 10E-6$	700	[42b]
Cytochrome c	Emitter	ITO/cytochrome c/Al	$6-8 \times 10E-6$	400	[42a]
Myoglobin	Emitter	ITO/myoglobin/Al	$1 \times 10E-5$	530–700	[42d]
Hemin	Emitter	ITO/hemin/Al	$1.73 \times 10E-5$	500–700	[42f]
Vitamin B12	Emitter	ITO/vitamin B12/Al	$3.6 \times 10E-6$	600–700	[42e]
RFLT	Emitter	ITO/PEDOT:PSS/PVK/RFLT/Ag	0.02	640	[45]
Chlorophyll a/b	Emitter	ITO/chlorophylls+PPV (carotenoids)/Al		680/660	[43]
DNA	Electron blocker	ITO/PEDOT:PSS/DNA/NPB/Alq3/BCP/Alq3/LiF/Al			[52a]
DNA–CTMA	Electron blocker	ITO/PEDOT:PSS/DNA + 1.5 wt% NB/LiF/Al		650	[53]
DNA	Electron blocker	ITO/PEDOT:PSS/DNA/(PVK + 40 wt% PBD) + 2 wt% Ir(ppy)/LiF/Al		530	[53]
A,G,C,T,U (nucleobase)	Electron blocker	ITO/PEDOT:PSS/nucleobase/CBP:Ir(ppy)3/BCP/Alq3/LiF/Al	0.9–14.3		[54]
A,G,C,T,U (nucleobase)	Hole blocker	ITO/PEDOT:PSS/NPB/CBP:Ir(ppy)3/nucleobase/Alq3/LiF/Al	0.3–4.6		[54]
Adenine	Hole injection	Cellulose/epoxy/Au/Adenine/NPB/CBP:Ir(ppy)3/Alq3/BCPLiF/Al	510		[55]
DNA–BTMA DNA–CTMA	Electron blocker	ITO/PEDOT:PSS/DNA biopolymer/NPB/Alq3/LiF/Al	1.39–1.47	430	[56]
Eumelanin–PEDOT	Electrode	Glass/eumelanin–PEDOT/α-NPD/Alq3/Ca/Al			[66b]
AgNWs/alginate	Electrode	ITO/AgNWs/alginate/PEDOT:PSS/MoO₃/Mcp/Ir(tfmppy)2(tpip)/TPBi/LiF/Al			[65]

**ADVANCED
SCIENCE NEWS**
www.advancedsciencenews.com

**ADVANCED
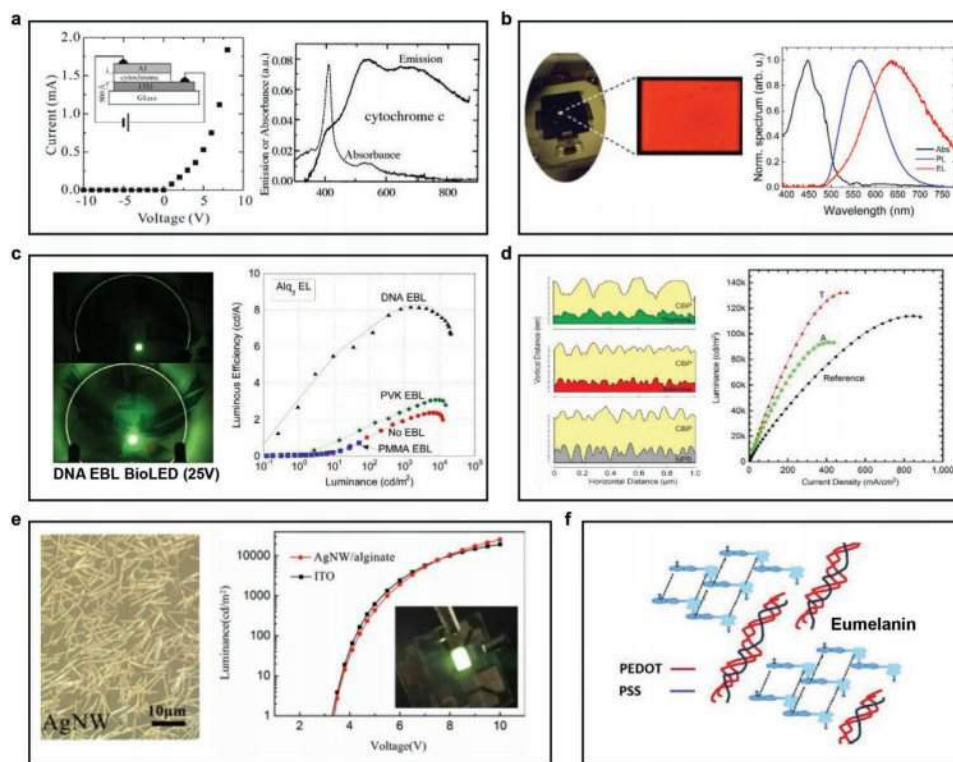MATERIALS
TECHNOLOGIES**
www.advmattechnol.de

Figure 5. a) (Left) Schematic of a typical organic light-emitting diode (OLED) structure (ITO/cytochrome c/Al) and the corresponding current–voltage characteristic, and (right) EL electroluminescence (EL) and absorption spectra of the cytochrome c film. Reproduced with permission.[42d] Copyright 2003, Elsevier. b) (Left) EL image of a vitamin-derived riboflavin tetrabutyrate OLED, and (right) absorbance (Abs), PL, and EL of the vitamin derived bio-OLED. Reproduced with permission.[45] Copyright 2017, American Chemical Society. c) (Left) EL emission of a DNA-based bio-LED, and (right) luminous efficiency versus luminance of the bio-LEDs with different electron blocking layers (EBLs). Reproduced with permission.[52a] Copyright 2006, American Institute of Physics. d) (Left) Morphologies of CBP films grown on different substrates (various electron blocking layers: thymine, adenine, and NPB), and (right) luminance versus current density for different devices. Reproduced with permission.[54b] Copyright 2014, Nature Publishing Group. e) (Left) Optical image of silver nanowires (AgNWs) on an alginate film, and (right) EL results for OLEDs on ITO and AgNW/alginate substrates. Reproduced with permission.[65] Copyright 2018, Wiley-VCH. f) Scheme of eumelanin embedded in PEDOT:PSS for OLED applications. Reproduced with permission.[66b] Copyright 2017, Wiley-VCH.

materials and related complexes have been extensively explored in previous research, owing to their unique electrical and optical properties.[47] Easily accessible from nature, properties of DNAs can be tuned by combining different lipid groups to become soluble in solvents and adhere to various substrates.[48] These DNA-based biomaterials are applied as the host of lumophores like rare-earth complexes and achieve efficiency improvements with further modifications.[49,50] For example, by integrating DNA with cetyltrimethylammonium (CTMA), the formed DNA–CTMA complex serve as an effective hole transport layer in OLEDs, owing to its shallow LUMO.[51] As shown in Figure 5c, such DNA–CTMA complex can also serve as an electron blocking layer and decrease the nonradiative carrier recombination, exhibiting notably improved photoemission for those DNA-containing BioLEDs, compared with conventional green and blue OLEDs without DNAs.[52] Except serves as electron blocking layer and emitting layer matrix,[53] DNA also works in other functional parts like transport layer. Using various nucleobases (A, G, C, T, U) as carrier transport or blocking layers in OLEDs, the device performance can be greatly improved (Figure 5d).[54] Another work reports OLEDs made by gold coated cellulose as semitransparent electrodes

combined with DNA-based hole injection layer.[55] Additionally, DNA-aromatic surfactant-based biopolymers are employed to decrease operation voltages of OLEDs and increase the device's luminous efficiency by 50%.[56] In all, these DNA-based biof-riendly materials exhibit desirable optoelectronic properties and are ideal substitutes for certain functional layers in OLEDs. It is worth mentioning that DNA materials used in these works are made from food industry byproducts, which is commercially available from salmon testes at a relatively low cost.[49,57] Manufacturing of these bioderived materials like DNA at scale is also feasible, for example, from cultured bacterial cells.[58]

Functional optical devices for implantable systems also require other components including substrates and electrodes with ideal mechanical softness and biocompatibility or fully degradability. Biodegradable supporting materials that can potentially be applied for clinical use include synthetic polymers such as PLGA and PCL,[9] as well as bioderived polymers such as hydrogels[59] and cellulose.[60] For example, cellulose derived from bacterial cellulose,[61] wood powders,[62] cellulose diacetate foil,[63] and composite nanocellulose can serve as substrates for LEDs. As for electrodes, stretchable and transparent conductive layers are formed using gold nanomeshes[64] and silver

**ADVANCED
SCIENCE NEWS**

www.advancedsciencenews.com

**ADVANCED
MATERIALS
TECHNOLOGIES**

www.advmattechnol.de

nanowires embedded into biocompatible alginate (Figure 5e).[65] Figure 5f presents a transparent and conductive film made by poly(3,4-ethylenedioxythiophene)-poly(styrenesulfonate) (PEDOT:PSS) mixed into eumelanin coatings that comprise a melanin pigment.[66] These electrodes based on gold, silver, and PEDOT:PSS exhibit ideal electrical conductivity and biocompatibility, but they are not fully dissolvable in biological environments. It is still highly demanded to develop transparent conductive layers made of biodegradable electrodes such as metals and polymers. Although fully biocompatible or biodegradable OLEDs have not realized and there is still plenty of room to improve their performance in terms of quantum yields, brightness and chronic stability, preliminary works have demonstrate the utility of OLEDs for optogenetic stimulations of neural activities in cultured cells, and these devices present stable light output after ultraviolet and ethanol sterilization.[67] With the inherent advantages like flexibility, biocompatibility, and adjustable dimensions, recently reported low power OLEDs also integrated with neural tissues and interact with genetically engineered light-sensitive opsins.[68] We envision that there will be more investigations about the development of OLED-based implantable systems for biomedical applications in the future research.

In comparison with OLEDs based on small organic molecules, emitters based on long chain conjugate polymers (polymer LEDs (PLEDs)) are more suitable for large-scale, low-cost production, and exhibit better thermal and moisture stability.[69] Recently, pixilated PLEDs that are compatible with magnetic resonance imaging have also been reported optogenetically stimulate nerve systems.[70] Biocompatible and biodegradable materials are also explored and incorporated in various PLEDs for improved performance and biointegration. One of common methods is to embed biomaterials into luminescent conjugated polymers. As shown in **Figure 6**a, biodegradable insulin fibrils enhance electron injection and balance the collection of carriers in PPF-based PLEDs, leading to a tenfold increase of the EL efficiency.[71] In addition, the bovine submaxilliary mucin (BSM) protein can be employed to increase water solubility and prevent aggregation in originally hydrophobic conjugated polymers, resulting in significantly improved EL (Figure 6b).[72] Similar to results discussed in Figure 5, the DNA–CTMA complex also serves as an effective electron blocking layer in poly[2-methoxy-5-(20-ethylhexoxy)-1,4-phenylene vinylene] (MEH-PPV) and poly[9,9-dioctyfuorene] (PFO)-based PLEDs for efficiency improvement.[73] The DNA–CTMA is also reported as an effective hole transport and electron blocking layer in white PLEDs by mixing MEH-PPV and PFO in the active emitter (Figure 6c).[74] Compared to reference PLEDs without the DNA complex, the luminance efficiencies are nearly doubled in both MEH-PPV and PFO-based PLEDs, by adding the DNA layer between the electrode and MEH-PPV (Figure 6d).[75] It should be noted that the biomaterials only serve as carrier transport or blocking layers in these reported PLEDs, and it is still a daunting task to replace or modify the active emitting layer with more biocompatible and even biodegradable polymers.

Unlike OLEDs and PLEDs, light-emitting electrochemical cells (LECs) provide a different mechanism for EL, based on electrically mobile ions formed by dissolving salts in ion transport polymer and emitter. Such working principle enhances the electrical conductivity of devices layers, improves the stability, and enables the device to operate at higher voltages. **Figure 7**a presents an LEC device based on the active emitter "Super Yellow" and a salt with conductive ions tetrabutylammonium tetrafluorborate (TBABF$_4$) embedded in a biodegradable matrix made by PLGA. The introduction of PLGA promotes the ionic conductivity and effectively reduces the turn-on voltage of devices.[76] Similarly, another biodegradable polymer PCL can also be applied as the host, achieving an LEC with similar performance (Figure 7b).[77] However, the
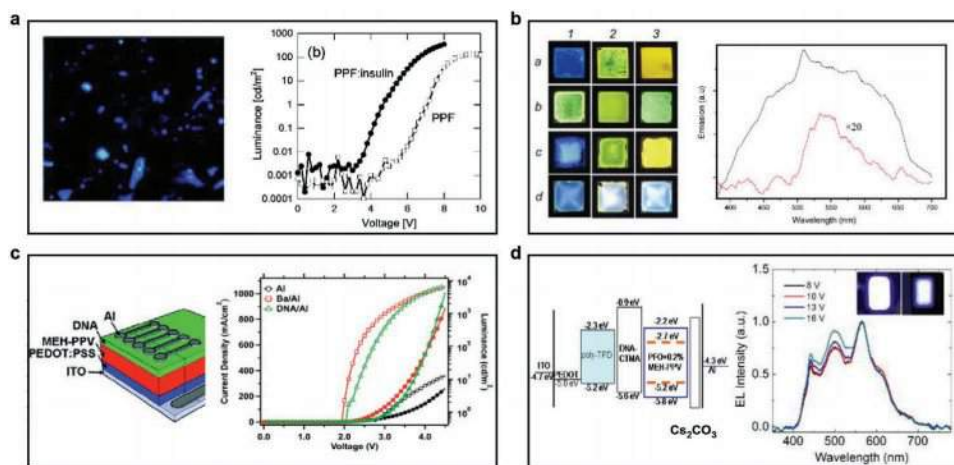

Figure 6. a) (Left) Fluorescence image of PPF:insulin fibril hybrid flim, and (right) luminance versus voltage of polymer LEDs (PLEDs) with and without insulin fibrils. Reproduced with permission.[71] Copyright 2008, American Chemical Society. b) (Left) PL images of different conjugated polymers, and (right) EL spectra for PLEDs with (black line) and without (red line) BSM in active layers. Reproduced with permission.[72] Copyright 2014, Wiley-VCH. c) (Left) Schematic for the PLED structure using DNA as electron injection interlayer, and (right) current density and luminance versus voltage for PLEDs with different electrodes. Reproduced with permission.[74] Copyright 2011, American Chemical Society. d) (Left) Schematic diagram of energy levels showing different layers in the DNA–CTMA-based PLED, and (right) normalized EL spectra of the PLED, the insets are photographs of PLEDs with and without designed blocking layers. Reproduced with permission.[75] Copyright 2008, American Institute of Physics.
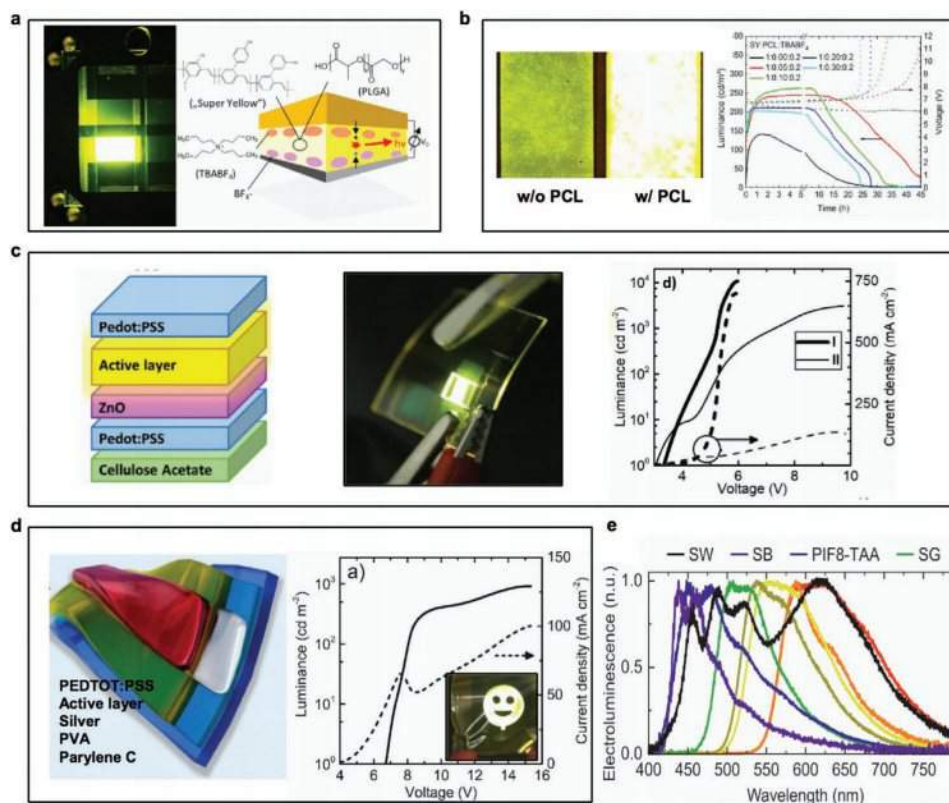
Figure 7. a) (Left) Image of a degradable light-emitting electrochemical cell (LEC), and (right) scheme of the LEC, with the active layer made of Super Yellow embedded in ion-conducting polymer PLGA. Reproduced with permission.[76] Copyright 2016, American Chemical Society. b) (Left) EL images for LECs with and without PCL, and (right) luminance and voltage versus time for LECs with different PCL concentrations. Reproduced with permission.[77] Copyright 2016, Nature Publishing Group. c) (Left) Structure of an LEC based on fully printed material layers on a degradable cellulose acetate substrate, (middle) EL image of the LEC, and (right) luminance and current density versus voltage curves for LECs with different structures. Reproduced with permission.[78] Copyright 2017, Wiley-VCH. d) (Left) Scheme of a fully printed flexible LEC, and (right) luminance and current density versus voltage curves for the flexible LEC (inset: the corresponding EL photograph). Reproduced with permission.[79] Copyright 2019, Wiley-VCH. e) Electroluminescence spectra of LECs with DNA–CTMA and eight electrochemical emitters. Reproduced with permission.[80] Copyright 2020, Wiley-VCH.

biocompatibility issue of the emitter (Super Yellow) and the salt $TBABF_4$ is unsolved in both works. In Figure 7c, a non-halogenated biodegradable solid electrolyte based on poly(ε-caprolactone-co-trimethylene carbonate) and tetrabutylammonium bis-oxalato borate is developed as the ion conductor in the LEC. In addition, the device is fabricated on a cellulose-based flexible biodegradable substrate. Compared with devices reported in Figure 7a,b, the resulted LEC achieves an order of magnitude increase in terms of the EL efficiency and luminescence.[78] Furthermore, fully printed and soft LECs based on the aforementioned biodegradable components are reported in Figure 7d.[79] DNA–CTMA is used in LECs as an ion-solvating component in solid polymer electrolyte and improves device performance owing to its great ionic dissociation and conductivity. Owing to its wide electrochemical window, DNA–CTMA could cooperate with different emitters covering the entire visible spectrum as shown in Figure 7e.[80] Although it is still challenging to realize a biodegradable active emitter without using the Super Yellow, these works provide a viable route to highly efficient, biocompatible and biodegradable LEC-based emitters.

4.2. Lead-Free Perovskite Materials and Devices

The abovementioned mentioned organic-based LEDs (OLEDs, PLEDs and LECs) are only partially biocompatible or biodegradable, with challenges including low electron-to-photon conversion efficiencies, low brightness, and lack of longtime stability. Recently, metal halide-based perovskite materials have attracted tremendous interests in the development of high performance optoelectronic devices including LEDs, solar cells, and photodetectors.[81] These perovskite materials are naturally water dissolvable, which makes them promising solutions to physically transient, degradable devices. However, most of the high performance LEDs are based on Pb halide perovskites,[14] which prohibit their use in environmental and biomedical applications.[82] Various metal elements are proposed and developed to replace Pb in the perovskite structure. Some possible candidate cations, including tellurium (Te^{4+})[83] and antimony (Sb^{3+}),[84] are less toxic than Pb but still not perfectly biocompatible. Other perovskites based on magnesium (Mg),[85] calcium (Ca),[86] and titanium (Ti)[87] are more promising and also explored. However, resulted perovskite materials are not ideal

Table 3. Material compositions, device structures, and optical performance for some representative Pb-free perovskite LEDs.

Perovskite materials	Device structure	EL peak [nm]	EQE [%]	Luminescence	Refs.
$(PEA)_2SnI_4$	Emitting	618		0.15 cd m^{-2} (6 V)	[102]
$(PEA)_2SnI_4$	ITO/PEDOT:PSS/2D perovskite/TPBi/LiF/Al	629	0.16	58 cd m^{-2}	[104]
$(TEA)_2SnI_4$	–	638	0.62	322 cd m^{-2}	[104]
$(PEAI)_x(CsI)_y(SnI_2)_z$	ITO/PVK/perovskite MQWs/TmPyPB/LiF/Al		3		[105]
$CH_3NH_3Sn(Br/I)_3$	PEDOT:PSS/perovskite/F8/Ca/Al	945	0.72	1.8 W sr^{-1} m^{-2}	[101]
$CsSnI_3$	PEDOT:PSS/perovskite/PBD/LiF/Al	950	3.8	40 W sr^{-1} m^{-2}	[100]
$(OCTAm)_2SnBr_4$	ZnO(PEI)/perovskite/TCTA/MoO$_3$/Au	635	0.1	350 cd m^{-2}	[103]
$(PEA)_2SnI_4$	ITO/PEDOT:PSS/perovskite/TPBi/LiF/Al	633	0.3	70 cd m^{-2} (5.8 V)	[106]
$(PEA)_2SnI_4$	ITO/PEDOT:PSS/perovskite + DSAS/TPBi/LiF/Al		0.72	132 cd m^{-2}	[107]
$Cs_3Cu_2I_5$	ITO/p-NiO/perovskite NCs/TPBi/LiF/Al	445	1.12	262.6 cd m^{-2} (7.5 V)	[115]
$CsCu_2I_3$	ITO/PEDOT:PSS/poly-TPD/perovskite/TPBi/LiF/Al	550	0.17	47.5 cd m^{-2}	[116b]
$CsCu_2I_3$	ITO/NiO$_x$/perovskite/TPBi/LiF/Al	560	0.02	10 cd m^{-2}	[116c]
$Cs_3Cu_2I_5$	ZSO/perovskite/NPD/MoO$_x$/Ag	440	–	–	[113]
$Cs_2Ag_{0.6}Na_{0.4}InCl_6$	ITO-PEIE/ZnO-PEIE/perovskite/TAPC/MoO$_3$/Al	552	–	–	[117b]

solutions to higher performance LEDs. In these perovskites, the small ion radius of Mg could not support stable perovskite structures;[88] the lack of lone pair electrons in Ca ions could cause a heavy effective mass of carriers;[86,88] and the vacancy-ordered double perovskites with Ti has quasi-direct bandgaps, leading to inefficient radiative recombinations.[87,89] Alternatively, biocompatible elements including germanium (Ge),[90] bismuth (Bi),[91] tin (Sn),[92] and copper (Cu)[93] may provide possible solutions to biodegradable perovskite LEDs. Biological toxicities and environmental impacts of these elements are analyzed and discussed in associated literature.[93–95] **Table 3** and **Figure 8** summarize material compositions, device structures and optoelectronic performance of representative perovskite LEDs based on Sn and Cu. As a group IV element, Sn is so far one of the most promising candidates for substitutes to Pb, since Sn-based halide perovskites own similar electronic structures with Pb-based ones, suitable bandgap and high carrier mobilities.[96] Efforts to realizing high performance Sn-based perovskite solar cells and LEDs have been focused on fabricating low-dimensional 2D, 1D, and 0D perovskites,[97] modulating quantum confinement,[98] and preventing the oxidation of Sn^{2+}.[99] The first reported Sn-based perovskite LED consists of compact micrometer-sized $CsSnI_3$ grains formed with the toluene dripping method, which dramatically decreases pinholes and cracks at grain boundaries. The fabricated infrared LED achieve a maximum EQE of 3.8%.[100] Another example demonstrates near-infrared LEDs with tunable bandgaps by adjusting ratio of halide in $CH_3NH_3Sn(Br_{1-x}I_x)_3$.[101] Low-dimensional Sn-based perovskite LEDs are also reported. Figure 8a presents 2D perovskite based on $(PEA)_2SnI_xBr_{4-x}$ (PEA: $C_6H_5CH_2CH_2NH_3^+$) incorporating PEA with a large ionic radius. Such a 2D structure helps exciton confinement and promotes radiative recombination, leading to a higher emission efficiency than their 3D counterparts.[102] Other low-dimensional Sn-based perovskites with different spacer cations present higher performance in LEDs including bright orange electroluminescent 2D[103] and 2D $(TEA)_2SnI_4$ (TEAI: 2-thiopheneethylamine iodide)

(Figure 8b).[104] Quantum well combined with 2D and 3D perovskite possess wider emission range, higher efficiency and longer life time.[105] Works focus on preventing Sn^{2+} oxidation are mainly adding stabilizers. Reducing agent H_3PO_2 forming complex with perovskite to hinder oxidation.[106] Apart from suppressing Sn^{2+} oxidation, additive naphthol sulfonic salt could modulate perovskite crystallization and passivate defects resulting in enhancement of device performance (Figure 8c).[107] Aside from Sn, Bi, Cu, Ag, and In are also investigated to replace Pb for high efficiency light emitters. Bi^{3+} has an electronic structure and ionic radius similar to Pb^{2+}. Stable $Cs_3Bi_2Br_9$-based perovskite QDs are synthesized (Figure 8d).[108,109] Although these QDs exhibit low quantum yields, they can be improved by further surface passivation.[110] In addition, Bi could be added as a dopant to Cs_2SnCl_6, leading to an enhanced PL efficiency.[111] Current works on Bi-based perovskites are still focused on their PL performance, Bi-based LEDs have not been reported so far. Cu-based perovskites have recently drawn considerable attention, owing to their low toxicity, facile synthesis, and relatively high radiative efficiency and stability.[112,113] Two types of Cu-based stable perovskites with different stoichiometries $CsCu_2X_3$ and $Cs_3Cu_2X_5$ (X = Cl, Br, I) are reported.[114] Figure 8e shows blue LEDs formed by solution processed $Cs_3Cu_2I_5$, and their efficiency could be further improved by employing proper carrier transport layers.[113] Further work reports $Cs_3Cu_2I_5$ nanocrystal-based deep blue LEDs with an external quantum efficiency of about 1.12%, which is comparable to state-of-the-art Pb-based perovskite blue LEDs. Moreover, the device holds a half lifetime reaching 108 h (Figure 8f).[115] Recent work also demonstrates $CsCu_2X_3$ LEDs with yellow emissions generated from self-trapped excitons (Figure 8g), and the devices avoid the phase separation occurring in Pb-based yellow emitting perovskite LEDs with mixed halides.[109,110,116] Double perovskites with $A_2B_IB_{II}X_6$ structures also show promise as high performance light emitters. For example, attempts to form doped $Cs_2AgInCl_6$ structures lead to materials with highly efficient PL based on self-trapped
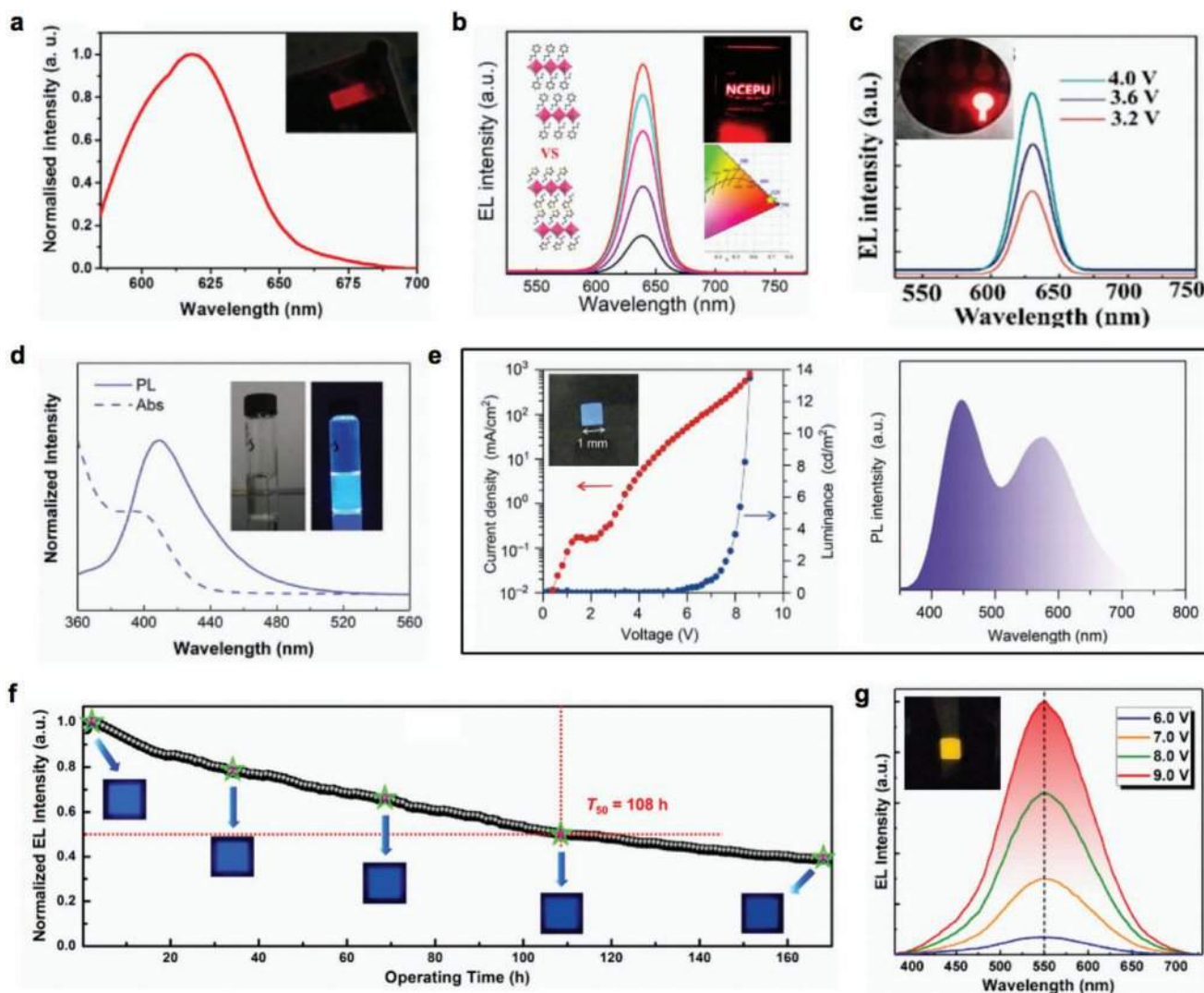
**ADVANCED
SCIENCE NEWS**

www.advancedsciencenews.com

**ADVANCED
MATERIALS
TECHNOLOGIES**

www.advmattechnol.de

Figure 8. a) EL spectrum of a 2D (PEA)$_2$SnI$_x$Br$_{4-x}$-based LED. Reproduced with permission.[102] Copyright 2017, American Chemical Society. b) Emission and structure of a 2D (PEA/TEA)$_2$SnI$_3$ LED. Reproduced with permission.[104] Copyright 2020, American Chemical Society. c) Emission of a 2D ((PEA)$_2$SnI$_4$) LED with naphthol sulfonic salt passivation. Reproduced with permission.[107] Copyright 2020, American Chemical Society. d) PL and absorption spectra of (CH$_3$NH$_3$)$_3$Bi$_2$ × 9 QDs. Reproduced with permission.[109] Copyright 2018, Wiley-VCH. e) (Left) Current density and luminance versus voltage for 0D Cs$_3$Cu$_2$I$_5$ LEDs, and (right) PL spectrum of the 0D Cs$_3$Cu$_2$I$_5$ crystals. Reproduced with permission.[113] Copyright 2018, Wiley-VCH. f) Time-dependent EL intensity of Cs$_3$Cu$_2$I$_5$ nanocrystals with long working time. Reproduced with permission.[115] Copyright 2020, American Chemical Society. g) EL spectra of CsCu$_2$I$_3$-based LEDs at different voltages. Reproduced with permission.[116b] Copyright 2020, American Chemical Society.

excitons.[117] Silver is considered harmless to human health, while the dose of indium is restricted by maximum exposure.[95] Although there are few reports about employing these Pb-free perovskites for biointegrated applications, it is envisioned that more results will appear in the near future, presenting devices with high performance and stability in a more biofriendly format.

4.3. Other Inorganic Light Emitting Materials and Devices

LEDs based on other biocompatible inorganic semiconductors are also promising solutions to forming biodegradable optoelectronic systems and under active investigation. Semiconductors based on II–VI group elements like zinc oxide (ZnO)[118] and zinc sulfide (ZnS)[119] exhibit direct gap transitions and show ultraviolet or blue emissions with decent quantum yields. With proper dopants of transition metals, their emission spectra can be further shifted to longer wavelengths (**Figure 9**a).[120] The doped ZnS NPs can be used to excite red emission sodium chlorophyllin copper salt, emulating the emission of chlorophyll in biological systems.[121] Water soluble, electrically driven light emitting devices are demonstrated, based on structures of a ZnS:Cu and ZnS:Cu,Mn-polyvinyl pyrrolidone (PVP) composite emitting layer and silver nanowire (AgNW) electrodes made via roll-to-roll production (Figure 9b).[122] The device exhibit bright white light EL; however, the operating voltages are higher than 50 V, limiting their use as wearable and implantable devices.
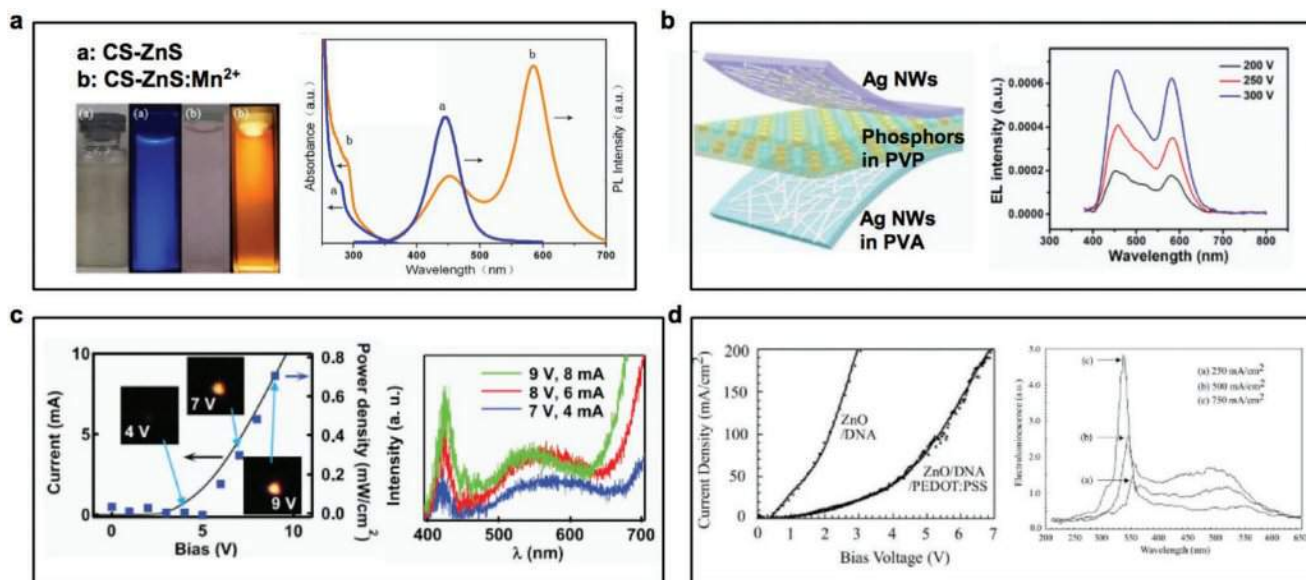
**ADVANCED
SCIENCE NEWS**
www.advancedsciencenews.com

**ADVANCED
MATERIALS
TECHNOLOGIES**
www.advmattechnol.de

Figure 9. a) (Left) Photographs of ZnS and ZnS:Mn^{2+} QDs under ambient light and UV excitations, and (right) PL and absorbance spectra of the corresponding ZnS QDs. Reproduced with permission.[120] Copyright 2011, Springer. b) (Left) Schematic illustration of the flexible transient alternating current EL device, and (right) EL spectra of the device at different voltages. Reproduced with permission.[122] Copyright 2018, Nature Publishing Group. c) (Left) Current and optical power density versus voltage curves of a fully transient ZnO-based LED, and (right) EL spectra of the ZnO LEDs at different voltages. Reproduced with permission.[124] Copyright 2019, Wiley-VCH. d) (Left) Current density versus voltage for ZnO-based UV LEDs, and (right) EL spectra of the ZnO UV LEDs. Reproduced with permission.[125] Copyright 2011, SPIE.

Similarly, an EL device based on ZnS phosphors are formed on a stretchable platform and show a reduced turn-on voltage (≈20 V), which enables their capability for use in wearable and soft robotic systems.[123] More recently, full degradable LEDs based on ZnO are reported.[124] As shown in Figure 9c, the transient LED is based on a ZnO emitting layer with molybdenum (Mo) and doped silicon (Si) as electrodes, resulting in a turn-on voltage of ≈5 V. Although there are plenty of works to improve the device performance in terms of its EL efficiency, operating voltage, brightness, and color quality, it provides a promising route to a fully biodegradable LED with ideal biocompatibility. Another work demonstrates ZnO nanorod-based LEDs with the salmon deoxyribonucleic acid (sDNA)–cetyltrimethylammonium complex as the electron blocking layer, which leads to a decreased operating voltage compared to a PEDOT:PSS-based electrode (Figure 9d).[125] In the future, these inorganic LEDs based on biodegradable emitters would be utilized for in vivo applications such as optogenetically modulate brain, spinal, and peripheral neural circuits, as demonstrated with traditional III–V semiconductor-based LEDs.[6,126]

5. Conclusions

To summarize, biocompatible and biodegradable light-emitting materials and devices are one of the key missing components in fully physically transient optoelectronics, which are particularly desirable for implantable systems with biomedical functionalities, including optogenetic modulation, photodynamic therapy, optical-based biosensing, etc. Biocompatible and even degradable light emitters with photoluminescence, mechanoluminescence, chemiluminescence, and bioluminescence have

been successfully applied in biological systems and even clinical uses, with remarkable examples including various luminescent dyes and proteins. Nevertheless, fully biodegradable high performance EL devices still remain as a daunting challenge. Ultimate goals are the development of fully degradable LEDs with desirable emission spectra and performance that is on par with state-of-the-art organic, perovskite and even inorganic III–V devices. In addition, all the device components, including active emitters, carrier blocking/transport layers, electrodes, as well as substrates and encapsulations, have to meet the stringent requirements for implantable uses. Among these functional layers, the active emitter material is the most essential component. Aside from the employment of conventional organic-, perovskite-, III–V-, and II–V-based materials, new options for semiconductors with high electron-to-photon conversion efficiencies and that can be safety absorbed within the body should be further exploited. In order to realize a high performance and fully biodegradable LED for implants, possible directions include: 1) modify conventional photoluminescent dyes or proteins and make them become electroluminescent; 2) band engineer biodegradable semiconductors like Pd-free perovskites, ZnO, and Si to improve their EL efficiencies; 3) explore novel OLEDs and PLEDs that are more biocompatible and degradable. Upon successful realization of the active emitters, the development of a fully biocompatible and biodegradable LED would be readily viable, considering other functional parts, like electrodes (Mg, Zn, etc.), carrier transfer/blocking layers (DNA, etc.), and substrates (hydrogels, PLGA, etc.), are widely available. We envision that the exploration of such biocompatible and biodegradable light emitters and devices would establish the foundations of transient device systems, and create vast opportunities for biological applications and medical practice.

Acknowledgements

Conflict of Interest

The authors declare no conflict of interest.

Keywords

[1] a) Y. Xue, S. Q. Shen, J. C. Corbo, V. J. Kefalov, *Sci. Rep.* **2015**, *5*, 17616; b) T. Liu, J. Jiao, X. Xu, X. Liu, S. Deng, S. Liu, *Proc. SPIE* **2005**, *5630*, 185; c) J. W. Hastings, *Ciba Found. Symp.* **1975**, *31*, 125.

[2] a) H. Zhu, P. Cheng, P. Chen, K. Pu, *Biomater. Sci.* **2018**, *6*, 746; b) S. H. Yun, S. J. J. Kwok, *Nat. Biomed. Eng.* **2017**, *1*, 0008; c) J. V. Frangioni, *Curr. Opin. Chem. Biol.* **2003**, *7*, 626.

[3] a) K. Kwon, T. Son, K.-J. Lee, B. Jung, *Lasers Med. Sci.* **2009**, *24*, 605; b) A. Canales, X. Jia, U. P. Froriep, R. A. Koppes, C. M. Tringides, J. Selvidge, C. Lu, C. Hou, L. Wei, Y. Fink, P. Anikeeva, *Nat. Biotechnol.* **2015**, *33*, 277.

[4] a) J. Yoon, S. Lee, D. Kang, M. Meitl, C. Bower, J. A. Rogers, *Adv. Opt. Mater.* **2015**, *3*, 1313; b) E. Song, C.-H. Chiang, R. Li, X. Jin, J. Zhao, M. Hill, Y. Xia, L. Li, Y. Huang, S. M. Won, K. J. Yu, X. Sheng, H. Fang, M. A. Alam, Y. Huang, J. Viventi, J.-K. Chang, J. A. Rogers, *Proc. Natl. Acad. Sci. USA* **2019**, *116*, 15398.

[5] G. Shin, A. M. Gomez, R. Al-Hasani, Y. R. Jeong, J. Kim, Z. Xie, A. Banks, S. M. Lee, S. Y. Han, C. J. Yoo, J.-L. Lee, S. H. Lee, J. Kurniawan, J. Tureb, Z. Guo, J. Yoon, S.-I. Park, S. Y. Bang, Y. Nam, M. C. Walicki, V. K. Samineni, A. D. Mickle, K. Lee, S. Y. Heo, J. G. McCall, T. Pan, L. Wang, X. Feng, T.-i. Kim, J. K. Kim, Y. Li, Y. Huang, R. W. Gereau, J. S. Ha, M. R. Bruchas, J. A. Rogers, *Neuron* **2017**, *93*, 509.

[6] H. Zhang, P. Gutruf, K. Meacham, M. C. Montana, X. Zhao, A. M. Chiarelli, A. Vázquez-Guardado, A. Norris, L. Lu, Q. Guo, C. Xu, Y. Wu, H. Zhao, X. Ning, W. Bai, I. Kandela, C. R. Haney, D. Chanda, R. W. Gereau, J. A. Rogers, *Sci. Adv.* **2019**, *5*, eaaw0873.

[7] S.-K. Kang, J. Koo, Y. K. Lee, J. A. Rogers, *Acc. Chem. Res.* **2018**, *51*, 988.

[8] L. Yin, H. Cheng, S. Mao, R. Haasch, Y. Liu, X. Xie, S.-W. Hwang, H. Jain, S.-K. Kang, Y. Su, R. Li, Y. Huang, J. A. Rogers, *Adv. Funct. Mater.* **2014**, *24*, 645.

[9] S. W. Hwang, J. K. Song, X. Huang, H. Cheng, S. K. Kang, B. H. Kim, J. H. Kim, S. Yu, Y. Huang, J. A. Rogers, *Adv. Mater.* **2014**, *26*, 3905.

[10] A. Sannino, C. Demitri, M. Madaghiele, *Materials* **2009**, *2*, 353.

[11] S.-K. Kang, G. Park, K. Kim, S.-W. Hwang, H. Cheng, J. Shin, S. Chung, M. Kim, L. Yin, J. C. Lee, K.-M. Lee, J. A. Rogers, *ACS Appl. Mater. Interfaces* **2015**, *7*, 9297.

[12] a) K. K. Fu, Z. Wang, J. Dai, M. Carter, L. Hu, *Chem. Mater.* **2016**, *28*, 3527; b) R. Li, L. Wang, D. Kong, L. Yin, *Bioact. Mater.* **2018**, *3*, 322.

[13] a) E. Fresta, V. Fernández-Luna, P. B. Coto, R. D. Costa, *Adv. Funct. Mater.* **2018**, *28*, 1707011; b) W. Li, Q. Liu, Y. Zhang, C. Li, Z. He, W. C. H. Choy, P. J. Low, P. Sonar, A. K. K. Kyaw, *Adv. Mater.* **2020**, *32*, 2001591.

[14] S. Nakamura, M. R. Krames, *Proc. IEEE* **2013**, *101*, 2211.

[15] a) K. Lin, J. Xing, L. N. Quan, F. P. G. de Arquer, X. Gong, J. Lu, L. Xie, W. Zhao, D. Zhang, C. Yan, W. Li, X. Liu, Y. Lu, J. Kirman, E. H. Sargent, Q. Xiong, Z. Wei, *Nature* **2018**, *562*, 245; b) M. S. White, M. Kaltenbrunner, E. D. Głowacki, K. Gutnichenko, G. Kettlgruber, I. Graz, S. Aazou, C. Ulbricht, D. A. M. Egbe, M. C. Miron, Z. Major, M. C. Scharber, T. Sekitani, T. Someya, S. Bauer, N. S. Sariciftci, *Nat. Photonics* **2013**, *7*, 811.

[16] R. Sjoback, J. Nygren, M. Kubista, *Spectrochim. Acta, Part A* **1995**, *51*, L7.

[17] H. Qi, C. Chang, L. Zhang, *Green Chem.* **2009**, *11*, 177.

[18] Y. H. Tsou, X. Q. Zhang, X. Bai, H. Zhu, Z. Li, Y. Liu, J. Shi, X. Xu, *Adv. Funct. Mater.* **2018**, *28*, 1802607.

[19] Y. Du, Y. Xue, P. Ma, X. Chen, B. Lei, *Adv. Healthcare Mater.* **2016**, *5*, 382.

[20] a) Y. Zhang, J. Yang, *J. Mater. Chem. B* **2013**, *1*, 132; b) Y. Sun, A. Periasamy, *Fluorescence Microscopy Imaging in Biomedical Sciences*, Springer, Berlin **2013**, pp. 79–110; c) T. Craggs, *Chem. Soc. Rev.* **2009**, *38*, 2865; d) M. Chalfie, Y. Tu, G. Euskirchen, W. W. Ward, D. C. Prasher, *Science* **1994**, *263*, 802;

[21] C. P. Carlos, S. F. Correia, M. Martins, O. A. Savchuk, J. A. Coutinho, P. S. André, J. B. Nieder, S. P. Ventura, R. A. Ferreira, *Green Chem.* **2020**, *22*, 4943.

[22] G. Gotthard, D. von Stetten, D. Clavel, M. Noirclerc-Savoye, A. Royant, *Biochemistry* **2017**, *56*, 6418.

[23] L. Tian, S. A. Hires, T. Mao, D. Huber, M. E. Chiappe, S. H. Chalasani, L. Petreanu, J. Akerboom, S. A. McKinney, E. R. Schreiter, C. I. Bargmann, V. Jayaraman, K. Svoboda, L. L. Looger, *Nat. Methods* **2009**, *6*, 875.

[24] F. Sun, J. Zeng, M. Jing, J. Zhou, J. Feng, S. F. Owen, Y. Luo, F. Li, H. Wang, T. Yamaguchi, Z. Yong, Y. Gao, W. Peng, L. Wang, S. Zhang, J. Du, D. Lin, M. Xu, A. C. Kreitzer, G. Cui, Y. Li, *Cell* **2018**, *174*, 481.

[25] a) V. Fernández-Luna, J. Fernández-Blázquez, M. Monclús, F. Rojo, R. Daza, D. Sanchez-deAlcazar, A. Cortajarena, R. Costa, *Mater. Horiz.* **2020**, *7*, 1790.; b) V. Fernandez-Luna, C. Pedro, R. Costa, *Angew. Chem., Int. Ed.* **2018**, *57*, 8826; c) M. Weber, L. Niklaus, M. Pröschel, P. Coto, U. Sonnewald, R. Costa, *Adv. Mater.* **2015**, *27*, 5493.

[26] a) H. Jia, Z. Wang, T. Yuan, F. Yuan, X. Li, Y. Li, Z. Tan, L. Fan, S. Yang, *Adv. Sci.* **2019**, *6*, 1900397; b) D. Jin, P. Xi, B. Wang, L. Zhang, J. Enderlein, A. Oije, *Nat. Methods* **2018**, *15*, 415.

[27] Y. Wang, A. Hu, *J. Mater. Chem. C* **2014**, *2*, 6921.

[28] a) Y. Song, S. Zhu, S. Zhang, Y. Fu, L. Wang, X. Zhao, B. Yang, *J. Mater. Chem. C* **2015**, *3*, 5976; b) S. Tao, S. Zhu, T. Feng, C. Xia, Y. Song, B. Yang, *Mater. Today Chem.* **2017**, *6*, 13.

[29] J. Schneider, C. J. Reckmeier, Y. Xiong, M. von Seckendorff, A. S. Susha, P. Kasák, A. L. Rogach, *J. Mater. Chem. C* **2017**, *121*, 2014.

[30] a) C. H. Wang, A. S. W. Wong, G. W. Ho, *Langmuir* **2007**, *23*, 11960; b) Z. L. Wang, *J. Phys.: Condens. Matter* **2004**, *16*, R829; c) Z. Zhang, H. Xiong, *Materials* **2015**, *8*, 3101.

[31] a) K. Kocsis, M. Niedermaier, J. Bernardi, T. Berger, O. Diwald, *Surf. Sci.* **2016**, *652*, 253; b) X. Gao, Y. Cui, R. Levenson, L. Chung, S. Nie, *Nat. Biotechnol.* **2004**, *22*, 969.

[32] E. Moyen, J. Kim, J. Kim, J. Jang, *ACS Appl. Nano Mater.* **2020**, *3*, 5203.

[33] W. Shao, G. Chen, A. N. Kuzmin, H. L. Kutscher, A. Pliss, T. Y. Ohulchanskyy, P. N. Prasad, *J. Am. Chem. Soc.* **2016**, *138*, 16192.

[34] R. Canaparo, F. Foglietta, F. Giuntini, A. Francovich, L. Serpe, *Photochem. Photobiol. Sci.* **2020**, *19*, 1114.

[35] R. D. C. Soltani, M. Mashayekhi, M. Naderi, G. Boczkaj, S. Jorfi, M. Safari, *Ultrason. Sonochem.* **2019**, *55*, 117.

[36] E. H. White, O. Zafiriou, H. H. Kagi, J. H. Hill, *J. Am. Chem. Soc.* **1964**, *86*, 940.

[37] a) D. Mao, W. Wu, S. Ji, C. Chen, F. Hu, D. Kong, D. Ding, B. Liu, *Chem* **2017**, *3*, 991; b) C. M. Magalhaes, J. C. Esteves da Silva, L. Pinto da Silva, *ChemPhysChem* **2016**, *17*, 2286.

[38] a) T. Noguchi, S. Golden, Bioluminescent and Fluorescent Reporters in Circadian Rhythm Studies **2017**, http://ccb.ucsd.edu/the-bioclock-studio/education-resources/reporter-review/index.html (accessed: February 2021); b) V. Viviani, T. Oehlmeyer, F. Arnoldi, M. Brochetto-Braga, *Photochem. Photobiol.* **2005**, *81*, 843.

[39] S. Iwano, M. Sugiyama, H. Hama, A. Watakabe, N. Hasegawa, T. Kuchimaru, K. Z. Tanaka, M. Takahashi, Y. Ishida, J. Hata, S. Shimozono, K. Namiki, T. Fukano, M. Kiyama, H. Okano, S. Kizaka-Kondoh, T. J. McHugh, T. Yamamori, H. Hioki, S. Maki, A. Miyawaki, *Science* **2018**, *359*, 935.

[40] T. Mitiouchkina, A. S. Mishin, L. G. Somermeyer, N. M. Markina, T. V. Chepurnyh, E. B. Guglya, T. A. Karataeva, K. A. Palkina, E. S. Shakhova, L. I. Fakhranurova, S. V. Chekova, A. S. Tsarkova, Y. V. Golubev, V. V. Negrebetsky, S. A. Dolgushin, P. V. Shalaev, D. Shlykov, O. A. Melnik, V. O. Shipunova, S. M. Deyev, A. I. Bubyrev, A. S. Pushin, V. V. Choob, S. V. Dolgov, F. A. Kondrashov, I. V. Yampolsky, K. S. Sarkisyan, *Nat. Biotechnol.* **2020**, *38*, 944.

[41] a) H. Ding, L. Lu, Z. Shi, D. Wang, L. Li, X. Li, Y. Ren, C. Liu, D. Cheng, H. Kim, N. C. Giebink, X. Wang, L. Yin, L. Zhao, M. Luo, X. Sheng, *Proc. Natl. Acad. Sci. USA* **2018**, *115*, 6632; b) J. Kim, G. A. Salvatore, H. Araki, A. M. Chiarelli, Z. Xie, A. Banks, X. Sheng, Y. Liu, J. W. Lee, K.-I. Jang, S. Y. Heo, K. Cho, H. Luo, B. Zimmerman, J. Kim, L. Yan, X. Feng, S. Xu, M. Fabiani, G. Gratton, Y. Huang, U. Paik, J. A. Rogers, *Sci. Adv.* **2016**, *2*, e1600418; c) Z. Liu, W. C. Chong, K. M. Wong, K. M. Lau, *Microelectron. Eng.* **2015**, *148*, 98; d) C. Gobler, C. Bierbrauer, R. Moser, M. Kunzer, K. Holc, W. Pletschen, K. Köhler, J. Wagner, M. Schwaerzle, P. Ruther, O. Paul, J. Neef, D. Keppeler, G. Hoch, T. Moser, U. T. Schwarz, *J. Phys. D: Appl. Phys.* **2014**, *47*, 205401.

[42] a) S. Ikeda, H. Tajima, M. Matsuda, Y. Ando, H. Akiyama, *Bull. Chem. Soc. Jpn.* **2005**, *78*, 1608; b) K. Shimatani, H. Tajima, T. Komino, S. Ikeda, M. Matsuda, Y. Ando, H. Akiyama, *Chem. Lett.* **2005**, *34*, 948; c) H. Tajima, S. Ikeda, M. Matsuda, N. Hanasaki, J.-W. Oh, H. Akiyama, *Solid State Commun.* **2003**, *126*, 579; d) H. Tajima, S. Ikeda, K. Shimatani, M. Matsuda, Y. Ando, J. Oh, H. Akiyama, *Synth. Met.* **2005**, *153*, 29; e) H. Tajima, K. Shimatani, T. Komino, S. Ikeda, M. Matsuda, Y. Ando, H. Akiyama, *Colloids Surf., A* **2006**, *61*, 284; f) H. Tajima, K. Shimatani, T. Komino, M. Matsuda, S. Ikeda, Y. Ando, H. Akiyama, *Bull. Chem. Soc. Jpn.* **2006**, *79*, 549.

[43] N. Ohtani, N. Kitagawa, T. Matsuda, *Jpn. J. Appl. Phys.* **2011**, *50*, 01BC08.

[44] X. Li, X. Qin, H. Zheng, H. Yuan, Y. Guo, D. Xiao, *Electrochem. Commun.* **2015**, *61*, 66.

[45] N. Jürgensen, M. Ackermann, T. Marszalek, J. Zimmermann, A. J. Morfa, W. Pisula, U. H. F. Bunz, F. Hinkel, G. Hernandez-Sosa, *ACS Sustainable Chem. Eng.* **2017**, *5*, 5368.

[46] J. Richtar, P. Heinrichova, D. H. Apaydin, V. Schmiedova, C. Yumusak, A. Kovalenko, M. Weiter, N. S. Sariciftci, J. Krajcovic, *Molecules* **2018**, *23*, 2271.

[47] a) A. J. Steckl, *Nat. Photonics* **2007**, *1*, 3; b) J. G. Grote, J. A. Hagen, J. S. Zetts, R. L. Nelson, D. E. Diggs, M. O. Stone, P. P. Yaney, E. Heckman, C. Zhang, W. H. Steier, A. K. Y. Jen, L. R. Dalton, N. Ogata, M. J. Curley, S. J. Clarson, F. K. Hopkins, *J. Phys. Chem. B* **2004**, *108*, 8584.

[48] Y. Okahata, T. Kobayashi, K. Tanaka, M. Shimomura, *J. Am. Chem. Soc.* **1998**, *120*, 6165.

[49] N. Kobayashi, S. Uemura, K. Kusabuka, T. Nakahira, H. Takahashi, *J. Mater. Chem.* **2001**, *11*, 1766.

[50] a) K. Nakamura, H. Minami, A. Sagara, N. Itamoto, N. Kobayashi, *J. Mater. Chem. C* **2018**, *6*, 4516; b) K. Nakamura, T. Ishikawa, D. Nishioka, T. Ushikubo, N. Kobayashi, *Appl. Phys. Lett.* **2010**, *97*, 193301.

[51] K. Hirata, T. Oyamada, T. Imai, H. Sasabe, C. Adachi, T. Koyama, *Appl. Phys. Lett.* **2004**, *85*, 1627.

[52] a) J. A. Hagen, W. Li, A. J. Steckl, J. G. Grote, *Appl. Phys. Lett.* **2006**, *88*, 171109; b) A. J. Steckl, H. Spaeth, H. You, E. Gomez, J. Grote, *Opt. Photonics News* **2011**, *22*, 34.

[53] R. Grykien, B. Luszczynska, I. Glowacki, J. Ulanski, F. Kajzar, R. Zgarian, I. Rau, *Opt. Mater.* **2014**, *36*, 1027.

[54] a) E. F. Gomez, V. Venkatraman, J. G. Grote, A. J. Steckl, *Adv. Mater.* **2015**, *27*, 7552; b) E. F. Gomez, V. Venkatraman, J. G. Grote, A. J. Steckl, *Sci. Rep.* **2014**, *4*, 7105.

[55] E. F. Gomez, A. J. Steckl, *ACS Photonics* **2015**, *2*, 439.

[56] I. C. Chen, Y.-W. Chiu, Y.-C. Hung, *Jpn. J. Appl. Phys.* **2012**, *51*, 031601.

[57] a) E. Nowak, A. Wisła-Świder, G. Khachatryan, M. Fiedorowicz, K. Danel, *Eur. Biophys. J.* **2019**, *48*, 371; b) B. Sahraoui, M. Pranaitis, D. Gindre, J. Niziol, V. Kažukauskas, *J. Appl. Phys.* **2011**, *110*, 083117; c) V. Arasu, S. R. Dugasani, M. R. Kesama, H. K. Chung, S. H. Park, *Sci. Rep.* **2017**, *7*, 11567.

[58] A. Bodor, N. Bounedjoum, G. E. Vincze, Á. E. Kis, K. Laczi, G. Bende, Á. Szilágyi, T. Kovács, K. Perei, G. Rákhely, *Rev. Environ. Sci. Bio/Technol.* **2020**, *19*, 1.

[59] L. Li, J. Ge, B. Guo, P. X. Ma, *Polym. Chem.* **2014**, *5*, 2880.

[60] P. Le Rendu, T. P. Nguyen, L. Carrois, *Synth. Met.* **2003**, *138*, 285.

[61] a) E. R. P. Pinto, H. S. Barud, R. R. Silva, M. Palmieri, W. L. Polito, V. L. Calil, M. Cremona, S. J. L. Ribeiro, Y. Messaddeq, *J. Mater. Chem. C* **2015**, *3*, 11581; b) C. Legnani, H. S. Barud, J. M. A. Caiut, V. L. Calil, I. O. Maciel, W. G. Quirino, S. J. L. Ribeiro, M. Cremona, *J. Mater. Sci.: Mater. Electron.* **2019**, *30*, 16718; c) C. Legnani, C. Vilani, V. L. Calil, H. S. Barud, W. G. Quirino, C. A. Achete, S. J. L. Ribeiro, M. Cremona, *Thin Solid Films* **2008**, *517*, 1016.

[62] Y. Okahisa, A. Yoshida, S. Miyaguchi, H. Yano, *Compos. Sci. Technol.* **2009**, *69*, 1958.

[63] A. J. Morfa, T. Rödlmeier, N. Jürgensen, S. Stolz, G. Hernandez-Sosa, *Cellulose* **2016**, *23*, 3809.

[64] C. F. Guo, Q. Liu, G. Wang, Y. Wang, Z. Shi, Z. Suo, C.-W. Chu, Z. Ren, *Proc. Natl. Acad. Sci. USA* **2015**, *112*, 12332.

[65] L. Lian, D. Dong, D. Feng, G. He, *SID Int. Symp. Dig. Tech. Pap.* **2018**, *49*, 471.

[66] a) S. Tanpichai, S. K. Biswas, S. Witayakran, H. Yano, *Composites, Part A* **2020**, *132*, 105811; b) L. Migliaccio, S. Aprano, L. Iannuzzi, M. G. Maglione, P. Tassini, C. Minarini, P. Manini, A. Pezzella, *Adv. Electron. Mater.* **2017**, *3*, 1600342.

[67] J. T. Smith, B. O'Brien, Y.-K. Lee, E. J. Bawolek, J. B. Christen, *J. Disp. Technol.* **2014**, *10*, 514.

[68] A. Sridharan, A. Shah, S. S. Kumar, J. Kyeh, J. Smith, J. Blain-Christen, J. Muthuswamy, *Biomed. Phys. Eng. Express* **2020**, *6*, 025003.

[69] C. M. Carter, J. Cho, A. Glanzer, N. Kamcev, D. M. O'Carroll, *J. Cleaner Prod.* **2016**, *137*, 1418.

[70] a) B. F. E. Matarèse, P. L. C. Feyen, J. C. de Mello, F. Benfenati, *Front. Bioeng. Biotechnol.* **2019**, *7*, 278; b) D. Kim, T. Yokota, T. Suzuki, S. Lee, T. Woo, W. Yukita, M. Koizumi, Y. Tachibana, H. Yawo, H. Onodera, M. Sekino, T. Someya, *Proc. Natl. Acad. Sci. USA* **2020**, *117*, 21138.

[71] H. Tanaka, A. Herland, L. J. Lindgren, T. Tsutsui, M. R. Andersson, O. Inganäs, *Nano Lett.* **2008**, *8*, 2858.

[72] N. Hendler, J. Wildeman, E. D. Mentovich, T. Schnitzler, B. Belgorodsky, D. K. Prusty, D. Rimmerman, A. Herrmann, S. Richter, *Macromol. Biosci.* **2014**, *14*, 320.

[73] D. Madhwal, S. S. Rait, A. Verma, A. Kumar, P. K. Bhatnagar, P. C. Mathur, M. Onoda, *J. Lumin.* **2010**, *130*, 331.

[74] P. Zalar, D. Kamkar, R. Naik, F. Ouchen, J. G. Grote, G. C. Bazan, T. Q. Nguyen, *J. Am. Chem. Soc.* **2011**, *133*, 11010.

[75] Q. Sun, D. W. Chang, L. Dai, J. Grote, R. Naik, *Appl. Phys. Lett.* **2008**, *92*, 251108.

[76] J. Zimmermann, N. Jürgensen, A. J. Morfa, B. Wang, S. Tekoglu, G. Hernandez-Sosa, *ACS Sustainable Chem.* **2016**, *4*, 7050.

[77] N. Jurgensen, J. Zimmermann, A. J. Morfa, G. Hernandez-Sosa, *Sci. Rep.* **2016**, *6*, 36643.

[78] J. Zimmermann, L. Porcarelli, T. Rödlmeier, A. Sanchez-Sanchez, D. Mecerreyes, G. Hernandez-Sosa, *Adv. Funct. Mater.* **2017**, *28*, 1705795.

[79] J. Zimmermann, S. Schlisske, M. Held, J.-N. Tisserant, L. Porcarelli, A. Sanchez-Sanchez, D. Mecerreyes, G. Hernandez-Sosa, *Adv. Mater. Technol.* **2019**, *4*, 1800641.

[80] S. Tekoglu, M. Held, M. Bender, G. N. Yeo, A. Kretzschmar, M. Hamburger, J. Freudenberg, S. Beck, U. H. F. Bunz, G. Hernandez-Sosa, *Adv. Sustainable Syst.* **2020**, 2000203, https://doi.org/10.1002/adsu.202000203.

[81] S. D. Stranks, H. J. Snaith, *Nat. Nanotechnol.* **2015**, *10*, 391.

[82] J. Li, H. L. Cao, W. B. Jiao, Q. Wang, M. Wei, I. Cantone, J. Lu, A. Abate, *Nat. Commun.* **2020**, *11*, 310.

[83] D. Ju, X. Zheng, J. Yin, Z. Qiu, B. Türedi, X. Liu, Y. Dang, B. Cao, O. F. Mohammed, O. M. Bakr, X. Tao, *ACS Energy Lett.* **2018**, *4*, 228.

[84] K. M. Boopathi, P. Karuppuswamy, A. Singh, C. Hanmandlu, L. Lin, S. A. Abbas, C. C. Chang, P. C. Wang, G. Li, C. W. Chu, *J. Mater. Chem. A* **2017**, *5*, 20843.

[85] J. Wang, J. Dong, F. Lu, C. Sun, Q. Zhang, N. Wang, *J. Mater. Chem. A* **2019**, *7*, 23563.

[86] J. I. Uribe, D. Ramirez, J. M. Osorio-Guillén, J. Osorio, F. Jaramillo, *J. Phys. Chem. C* **2016**, *120*, 16393.

[87] M.-G. Ju, M. Chen, Y. Zhou, H. F. Garces, J. Dai, L. Ma, N. P. Padture, X. C. Zeng, *ACS Energy Lett.* **2018**, *3*, 297.

[88] D. Ray, C. Clark, H. Q. Pham, J. Borycz, R. J. Holmes, E. S. Aydil, L. Gagliardi, *J. Phys. Chem. C* **2018**, *122*, 7838.

[89] a) D. Kong, D. Cheng, X. Wang, K. Zhang, H. Wang, K. Liu, H. Li, X. Sheng, L. Yin, *J. Mater. Chem. C* **2020**, *8*, 1591; b) M. Chen, M.-G. Ju, A. D. Carl, Y. Zong, R. L. Grimm, J. Gu, X. C. Zeng, Y. Zhou, N. P. Padture, *Joule* **2018**, *2*, 558.

[90] a) I. Kopacic, B. Friesenbichler, S. F. Hoefler, B. Kunert, H. Plank, T. Rath, G. Trimmel, *ACS Appl. Energy Mater.* **2018**, *1*, 343; b) L.-J. Chen, *RSC Adv.* **2018**, *8*, 18396.

[91] a) A. H. Slavney, T. Hu, A. M. Lindenberg, H. I. Karunadasa, *J. Am. Chem. Soc.* **2016**, *138*, 2138; b) L. Zhang, K. Wang, B. Zou, *ChemSusChem* **2019**, *12*, 1612.

[92] W.-F. Yang, F. Igbari, Y.-H. Lou, Z.-K. Wang, L.-S. Liao, *Adv. Energy Mater.* **2020**, *10*, 1902584.

[93] A. M. Elseman, A. E. Shalan, S. Sajid, M. M. Rashad, A. M. Hassan, M. Li, *ACS. Appl. Mater. Interfaces* **2018**, *10*, 11699.

[94] a) T. Zhu, Y. Yang, X. Gong, *ACS Appl. Mater. Interfaces* **2020**, *12*, 26776; b) A. E. Shalan, S. Kazim, S. Ahmad, *ChemSusChem* **2019**, *12*, 4116.

[95] G. Schileo, G. Grancini, *J. Mater. Chem. C* **2021**, *9*, 67.

[96] N. K. Noel, S. D. Stranks, A. Abate, C. Wehrenfennig, S. Guarnera, A.-A. Haghighirad, A. Sadhanala, G. E. Eperon, S. K. Pathak, M. B. Johnston, A. Petrozza, L. M. Herz, H. J. Snaith, *Energy Environ. Sci.* **2014**, *7*, 3061.

[97] a) C. Zhou, H. Lin, Y. Tian, Z. Yuan, R. Clark, B. Chen, L. J. van de Burgt, J. C. Wang, Y. Zhou, K. Hanson, Q. J. Meisner, J. Neu, T. Besara, T. Siegrist, E. Lambers, P. Djurovich, B. Ma, *Chem. Sci.* **2018**, *9*, 586; b) R. Chiara, Y. O. Ciftci, V. I. E. Queloz, M. K. Nazeeruddin, G. Grancini, L. Malavasi, *J. Phys. Chem. Lett.* **2020**, *11*, 618.

[98] J. T. Lin, C. C. Liao, C. S. Hsu, D. G. Chen, H. M. Chen, M. K. Tsai, P. T. Chou, C. W. Chiu, *J. Am. Chem. Soc.* **2019**, *141*, 10324.

[99] H. Hoshi, N. Shigeeda, T. Dai, *Mater. Lett.* **2016**, *183*, 391.

[100] W. L. Hong, Y. C. Huang, C. Y. Chang, Z. C. Zhang, H. R. Tsai, N. Y. Chang, Y. C. Chao, *Adv. Mater.* **2016**, *28*, 8029.

[101] M. L. Lai, T. Y. Tay, A. Sadhanala, S. E. Dutton, G. Li, R. H. Friend, Z. K. Tan, *J. Phys. Chem. Lett.* **2016**, *7*, 2653.

[102] L. Lanzetta, J. M. Marin-Beloqui, I. Sanchez-Molina, D. Ding, S. A. Haque, *ACS Energy Lett.* **2017**, *2*, 1662.

[103] X. Zhang, C. Wang, Y. Zhang, X. Zhang, S. Wang, M. Lu, H. Cui, S. V. Kershaw, W. W. Yu, A. L. Rogach, *ACS Energy Lett.* **2018**, *4*, 242.

[104] Z. Wang, F. Wang, B. Zhao, S. Qu, T. Hayat, A. Alsaedi, L. Sui, K. Yuan, J. Zhang, Z. Wei, Z. Tan, *J. Phys. Chem. Lett.* **2020**, *11*, 1120.

[105] Y. Wang, R. Zou, J. Chang, Z. Fu, Y. Cao, L. Zhang, Y. Wei, D. Kong, W. Zou, K. Wen, N. Fan, N. Wang, W. Huang, J. Wang, *J. Phys. Chem. Lett.* **2019**, *10*, 453.

[106] H. Liang, F. Yuan, A. Johnston, C. Gao, H. Choubisa, Y. Gao, Y. K. Wang, L. K. Sagar, B. Sun, P. Li, G. Bappi, B. Chen, J. Li, Y. Wang, Y. Dong, D. Ma, Y. Gao, Y. Liu, M. Yuan, M. I. Saidaminov, S. Hoogland, Z. H. Lu, E. H. Sargent, *Adv. Sci.* **2020**, *7*, 1903213.

[107] C. Gao, Y. Jiang, C. Sun, J. Han, T. He, Y. Huang, K. Yao, M. Han, X. Wang, Y. Wang, Y. Gao, Y. Liu, M. Yuan, H. Liang, *ACS Photonics* **2020**, *7*, 1915.

[108] Z. Z. Ma, Z. F. Shi, L. T. Wang, F. Zhang, D. Wu, D. W. Yang, X. Chen, Y. Zhang, C. X. Shan, X. J. Li, *Nanoscale* **2020**, *12*, 3637.

[109] M. Leng, Y. Yang, K. Zeng, Z. Chen, Z. Tan, S. Li, J. Li, B. Xu, D. Li, M. P. Hautzinger, Y. Fu, T. Zhai, L. Xu, G. Niu, S. Jin, J. Tang, *Adv. Funct. Mater.* **2018**, *28*, 1704446.

[110] a) M. Leng, Y. Yang, Z. Chen, W. Gao, J. Zhang, G. Niu, D. Li, H. Song, J. Zhang, S. Jin, J. Tang, *Nano Lett.* **2018**, *18*, 6076; b) B. Yang, J. Chen, F. Hong, X. Mao, K. Zheng, S. Yang, Y. Li, T. Pullerits, W. Deng, K. Han, *Angew. Chem., Int. Ed. Engl.* **2017**, *56*, 12471.

[111] Z. Tan, J. Li, C. Zhang, Z. Li, Q. Hu, Z. Xiao, T. Kamiya, H. Hosono, G. Niu, E. Lifshitz, Y. Cheng, J. Tang, *Adv. Funct. Mater.* **2018**, *28*, 1801131.

[112] a) Z. X. Zhang, C. Li, Y. Lu, X. W. Tong, F. X. Liang, X. Y. Zhao, D. Wu, C. Xie, L. B. Luo, *J. Phys. Chem. Lett.* **2019**, *10*, 5343; b) P. Cheng, L. Sun, L. Feng, S. Yang, Y. Yang, D. Zheng, Y. Zhao, Y. Sang, R. Zhang, D. Wei, W. Deng, K. Han, *Angew. Chem., Int. Ed. Engl.* **2019**, *58*, 16087.

[113] T. Jun, K. Sim, S. Iimura, M. Sasase, H. Kamioka, J. Kim, H. Hosono, *Adv. Mater.* **2018**, *30*, 1804547.

[114] P. Sebastia-Luna, J. Navarro-Alapont, M. Sessolo, F. Palazon, H. J. Bolink, *Chem. Mater.* **2019**, *31*, 10205.

[115] L. Wang, Z. Shi, Z. Ma, D. Yang, F. Zhang, X. Ji, M. Wang, X. Chen, G. Na, S. Chen, D. Wu, Y. Zhang, X. Li, L. Zhang, C. Shan, *Nano Lett.* **2020**, *20*, 3568.

[116] a) Y. Zhu, J. Zhu, H. Song, J. Huang, Z. Lu, G. Pan, *J. Rare Earths* **2020**, *39*, 374; b) Z. Ma, Z. Shi, C. Qin, M. Cui, D. Yang, X. Wang, L. Wang, X. Ji, X. Chen, J. Sun, D. Wu, Y. Zhang, X. J. Li, L. Zhang, C. Shan, *ACS Nano* **2020**, *14*, 4475; c) N. Liu, X. Zhao, M. Xia, G. Niu, Q. Guo, L. Gao, J. Tang, *J. Semicond.* **2020**, *41*, 052204.

[117] a) P. Han, X. Zhang, C. Luo, W. Zhou, S. Yang, J. Zhao, W. Deng, K. Han, *ACS Cent. Sci.* **2020**, *6*, 566; b) J. Luo, X. Wang, S. Li, J. Liu, Y. Guo, G. Niu, L. Yao, Y. Fu, L. Gao, Q. Dong, C. Zhao, M. Leng, F. Ma, W. Liang, L. Wang, S. Jin, J. Han, L. Zhang, J. Etheridge, J. Wang, Y. Yan, E. H. Sargent, J. Tang, *Nature* **2018**, *563*, 541; c) H. Arfin, J. Kaur, T. Sheikh, S. Chakraborty, A. Nag, *Angew. Chem., Int. Ed. Engl.* **2020**, *59*, 11307.

[118] M. S. Ghamsari, S. Alamdari, D. Razzaghi, M. Arshadi Pirlar, *J. Lumin.* **2019**, *205*, 508.

[119] X. Ma, J. Song, Z. Yu, *Thin Solid Films* **2011**, *519*, 5043.

[120] S.-Q. Chang, B. Kang, Y.-D. Dai, H.-X. Zhang, D. Chen, *Nanoscale Res. Lett.* **2011**, *6*, 591.

**ADVANCED
SCIENCE NEWS**

www.advancedsciencenews.com

**ADVANCED
MATERIALS
TECHNOLOGIES**

www.advmattechnol.de

[121] K. B. Lin, Y. H. Su, *Appl. Phys. B* **2013**, *113*, 351.

[122] Y. Chen, H. Lu, F. Xiu, T. Sun, Y. Ding, J. Liu, W. Huang, *Sci. Rep.* **2018**, *8*, 6408.

[123] Y. J. Tan, H. Godaba, G. Chen, S. T. M. Tan, G. Wan, G. Li, P. M. Lee, Y. Cai, S. Li, R. F. Shepherd, J. S. Ho, B. C. K. Tee, *Nat. Mater.* **2020**, *19*, 182.

[124] D. Lu, T. L. Liu, J. K. Chang, D. Peng, Y. Zhang, J. Shin, T. Hang, W. Bai, Q. Yang, J. A. Rogers, *Adv. Mater.* **2019**, *31*, 1902739.

[125] R. B. Gupta, S. Nagpal, S. Arora, P. K. Bhatnagar, P. C. Mathur, *J. Nanophotonics* **2011**, *5*, 059505.

[126] a) K. L. Montgomery, A. J. Yeh, J. S. Ho, V. Tsao, S. Mohan Iyer, L. Grosenick, E. A. Ferenczi, Y. Tanabe, K. Deisseroth, S. L. Delp, A. S. Poon, *Nat. Methods* **2015**, *12*, 969; b) A. D. Mickle, S. M. Won, K. N. Noh, J. Yoon, K. W. Meacham, Y. Xue, L. A. McIlvried, B. A. Copits, V. K. Samineni, K. E. Crawford, D. H. Kim, P. Srivastava, B. H. Kim, S. Min, Y. Shiuan, Y. Yun, M. A. Payne, J. Zhang, H. Jang, Y. Li, H. H. Lai, Y. Huang, S. I. Park, R. W. Gereau, J. A. Rogers, *Nature* **2019**, *565*, 361; c) S. I. Park, D. S. Brenner, G. Shin, C. D. Morgan, B. A. Copits, H. U. Chung, M. Y. Pullen, K. N. Noh, S. Davidson, S. J. Oh, J. Yoon, K. I. Jang, V. K. Samineni, M. Norman, J. G. Grajales-Reyes, S. K. Vogt, S. S. Sundaram, K. M. Wilson, J. S. Ha, R. Xu, T. Pan, T. I. Kim, Y. Huang, M. C. Montana, J. P. Golden, M. R. Bruchas, R. W. Gereau, J. A. Rogers, *Nat. Biotechnol.* **2015**, *33*, 1280; d) V. K. Samineni, A. D. Mickle, J. Yoon, J. G. Grajales-Reyes, M. Y. Pullen, K. E. Crawford, K. N. Noh, G. B. Gereau, S. K. Vogt, H. H. Lai, J. A. Rogers, R. W. Gereau, *Sci. Rep.* **2017**, *7*, 15865.

Deying Kong is a Ph.D. candidate in the School of Materials Science and Engineering at Tsinghua University, China, under the supervision of Prof. Lan Yin. Her current research interests involve Preparation, integration and application of new perovskite photoelectric materials. She received her Bachelor's degree (2017) Tsinghua University.

Lan Yin is currently working as an associate professor in the School of Materials Science and Engineering at Tsinghua University, China. She received her Bachelor's and Ph.D. degrees from Tsinghua University and Carnegie Mellon University, respectively. Her current research is focused on biodegradable materials and electronics targeting applications for environment and healthcare.
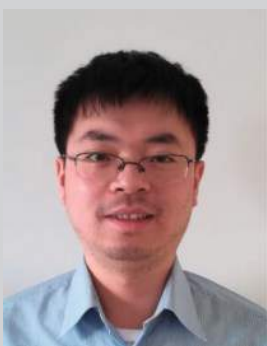
Xing Sheng is currently working as an associate professor in the Department of Electronic Engineering at Tsinghua University, China. He received his Bachelor's and Ph.D. degrees from Tsinghua University and Massachusetts Institute of Technology, respectively. His current research is focused on advanced optoelectronic materials, devices and systems for biomedical applications.